Chapter 2
Principles of Plasma Physics

The physics of plasmas are a special class of gasses made up of large number of electrons and ionized atoms and molecules, in addition to neutral atoms and molecules which are present in a non-ionized or so-called normal gas. Although by far most of the universe is ionized and is therefore in a plasma state, in our planet, plasmas have to be generated by special processes and under special conditions. Since human got to know fire and thunderstorm caused lighting in sky and the aurora borealis, we have been living in a bubble of essentially non-ionized gas in the midst of an otherwise, ionized environment. The physics of plasma is a field in which knowledge is expanding rapidly, in particular a means of producing what is so known as source generating clean energy via either magnetic confinement or inertial confinement. The growing science of plasmas excites lively interest in many people with various levels of training.

2.1 Introduction

Given the complexity of plasma behavior, the field of plasma physics is best described as a web of overlapping models, each based on a set of assumptions and approximations that make a limited range of behavior analytically and computationally tractable.

A conceptual view of the hierarchy of plasma models/approaches to plasma behavior that will be covered in this text is shown in Fig. 2.1. We will begin with the determination of individual particle trajectories in the presence of electric and magnetic fields.

Subsequently, it will be shown that the large number of charged particles in plasma facilitates the use of statistical techniques such as plasma kinetic theory, where the plasma is described by a velocity-space distribution function. Quite often, the kinetic theory approach retains more information than we really want

B. Zohuri, *Magnetic Confinement Fusion Driven Thermonuclear Energy*,
DOI 10.1007/978-3-319-51177-1_2

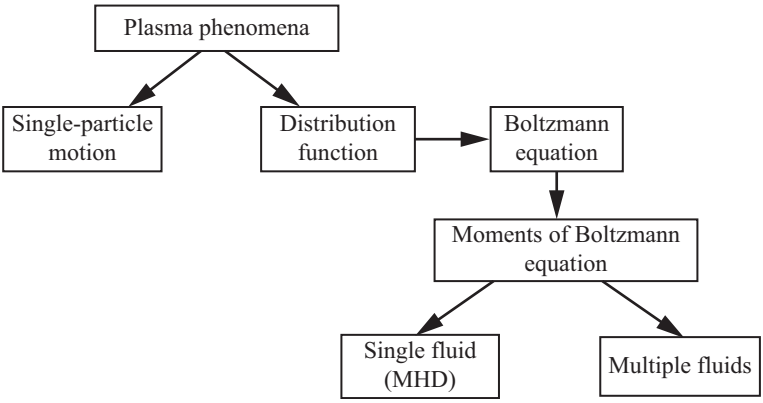

Fig. 2.1 Hierarchy of approach to plasma phenomena

about a plasma and a fluid approach better suited, in which only macroscopic variables (e.g., density, temperature, and pressure) are kept.

The combination of fluid theory with Maxwell's equations forms the basis of the field of magnetohydrodynamics (MHD), which is often used to describe the bulk properties and collective behavior of plasmas. The remainder of this chapter reviews important physical concepts and introduces basic properties of plasmas.

We have all learned from our high school science that matter appears in three states, namely:

1. Solid
2. Liquid
3. Gas

However, in recent years in particular after the explosion of thermonuclear weapon, scientists give more and more attention to the way of controlling the energy release from such weapon as new source of energy for our day-to-day use. Thus, their quest for new source of energy in a clean way (i.e., different than nuclear fission or coaled power plants) has taken them into different direction. This new direction has been toward controlled thermonuclear reactors, where deuterium (D) and tritium (T) fuse together to produce heavier nuclei such as helium and to liberate energy that can be found in our galaxy at the surface of in terrestrial universe. Therefore, for that reason, they have looked into properties of the fourth and unique state of matter, which is called *plasma*.

The higher the temperature, the more will be the freedom of the constituent particles of material experience.

In solid state of matter, the atoms and molecules are subject to strict solid and continuum mechanics discipline and are constructed to rigid order. In liquid form, matter can move, but their freedom is limited. However, at the gaseous stage, they can move freely, and from the viewpoint of quantum mechanics laws, inside the atoms, the electrons perform a harmonic motion over their orbits.

However, matter in plasma stage is highly ionized, and the electrons are liberated from atoms and acquire complete freedom of motion. Although plasma is often considered to be the fourth state of matter, it has many properties in common with the gaseous state. Meanwhile, the plasma is a fully ionized gas in which the long range of Coulomb forces gives rise to collective interaction effects, resembling a fluid with a density higher than that of a gas.

In its most general concept, plasma is any state of matter, which contains sufficient free, charged particles for its dynamic behavior to be dominated by electromagnetic forces. Since atomic nuclei are positively charged, when two nuclei are brought together as a preliminary to combination or fusion, there is an increasing force of electrostatic repulsion of their positive charges, which is described by Coulomb and defined as Coulomb force and results in some barrier that is known as Coulomb barrier.

In the fusion of light elements to form heavier ones, the nuclei (which carry positive electrical charge) must be forced close enough together to cause them to fuse into a single heavier nucleus. However, at a certain distance apart, the short-range nuclear attractive forces just exceed the long-range forces of repulsion, so the above fusion of the light elements becomes possible. The variation in the *potential energy* $V(r)$ of the system of two nuclei, with their distance r apart, is shown in Fig. 2.2.

Analyses of Fig. 2.2 indicate that a negative slope of potential energy curve presents net repulsion, whereas a positive slope implies net attraction. According to classical electromagnetic theory, the energy which must be supplied to the nuclei to surmount the Coulomb barrier, which is the amount of required energy to overcome the electrostatic repulsion so that fusion reaction can take place, is given by

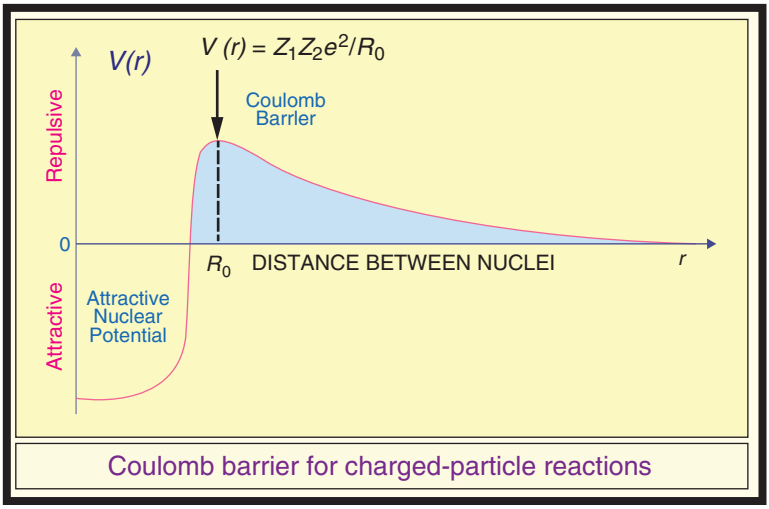

Fig. 2.2 Variation of Coulomb potential energy with distance between nuclei

$$V(r) = \frac{Z_1 Z_2 e^2}{R_0} \qquad \text{(Eq. 2.1)}$$

where:

$V(r)$ = potential energy to surmount Coulomb barrier
Z_1 = atomic number of nuclei element 1, carrying electric charge
Z_2 = atomic number of nuclei element 2, carrying electric charge
e = unit charge or proton charge
R_0 = distance between the centers of elements 1 and 2 at which the attractive forces become dominant

As it was stated in the previous text, Fig. 2.2 indicates that the force between nuclei is repulsive until a very small distance separates them, and then it rapidly becomes very attractive. Therefore, in order to surmount the Coulomb barrier and bring the nuclei close together where the strong attractive forces can be felt, the kinetic energy of the particles must be as high as the top of the Coulomb barrier.

In reality, effects associated with quantum mechanics help the situation. Because of what is termed the Heisenberg uncertainty principle, even if the particles do not have enough energy to pass over the barrier, there is a very small probability that the particles pass through the barrier. This is called barrier penetration or tunneling effect and is the means by which many such reactions take place in stars or terrestrial universe. Nevertheless, because this process happens with very small probability, the Coulomb barrier represents a strong hindrance to nuclear reactions in stars. Further discussion for barrier penetration can be found in next section.

The key to initiating a fusion reaction is for the nuclei to fuse to collide at very high velocities, thus driving them close enough together for the strong (but very short-ranged) nuclear forces to overcome the electrical repulsion between them. In stars, the temperature and the density at the center of the star govern the probability of this happening.

For light nuclei, which are of interest for controlled thermonuclear fusion reactions, R_0 may be taken as approximately equal to a nuclear diameter, i.e., 5×10^{-13} em; and since e is 4.80×10^{-10} esu (statcoulomb), it follows from Eq. 2.1 that

$$\begin{aligned} V(r) &= \frac{Z_1 Z_2 e^2}{R_0} \\ &= \frac{\left(4.80 \times 10^{-10}\right)^2 Z_1 Z_2}{5 \times 10^{-13}} \\ &= 4.6 \times 10^{-7} Z_1 Z_2 \\ &= 0.28 Z_1 Z_2 \ \text{MeV} \end{aligned} \qquad \text{(Eq. 2.2)}$$

where 1 MeV (million electron volts) is equivalent to 1.60×10^{-6} erg.

It is seen from Eq. 2.2 that the energy with the nuclei must be acquired before they can combine the increases with the atomic numbers Z_1 and Z_2, and even for reactions among the isotopes of hydrogen, namely, deuterium (D) and tritium (H), for which $Z_1 = Z_2 = 1$, the minimum energy, according to classical theory, is about 0.28 MeV. Even larger energies should be reactions involving nuclei of higher atomic number because of the increased electrostatic repulsion. Although energies of the order of magnitude indicated by Eq. 2.2 must be supplied to nuclei to cause them to combine fairly rapidly, experiments made with accelerated nuclei have shown that nuclear reactions can take place at detectable rates even when the energies are considerably below than those corresponding to the top of the Coulomb barrier.

In other words, we cannot determine the threshold energy, by the maximum electrostatic repulsion of the interacting nuclei, below which the fusion reaction will not occur. In such behavior, which cannot be explained by way of classical mechanics, however, it could be interpreted by means of wave mechanics [1].

2.2 Barrier Penetration

Classical physics reveals that a particle of energy E less than the height U_0 of barrier could not penetrate the region inside the barrier which is classically forbidden. However, the wave function associated with a free particle must be continuous at the barrier and will show an exponential decay inside the barrier. The wave function must also be continuous on the far side of the barrier, so there is a finite probability that the particle will tunnel through the barrier. See Fig. 2.3.

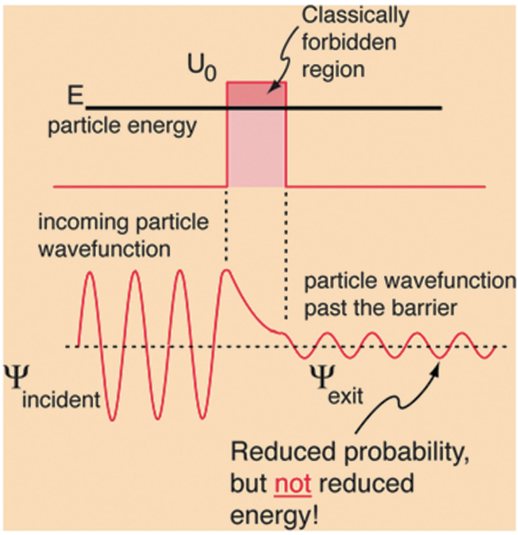

Fig. 2.3 Barrier penetration depiction

A free particle wave function in classical quantum mechanics is described as the particle approaches the barrier. When it reaches the barrier, it must satisfy the Schrödinger equation in the form of a quantum harmonic oscillator as

$$-\frac{\hbar^2}{2m}\frac{\partial^2\Psi(x)}{\partial x^2} = (E - U_0)\Psi(x) \qquad \text{(Eq. 2.3a)}$$

or

$$\frac{\partial^2\Psi(x)}{\partial x^2} + \frac{2m(E - U_0)}{\hbar^2}\Psi(x) = 0 \qquad \text{(Eq. 2.3b)}$$

Equation 2.3b which is a one-dimensional ordinary differential equation has the following solution as

$$\Psi(x) = A\mathrm{e}^{-\alpha x} \quad \text{where} \quad \alpha = \sqrt{\frac{2m(U_0 - E)}{\hbar^2}} \qquad \text{(Eq. 2.4)}$$

where $\hbar = h/2\pi$ is and h is Planck constant.

Note that in addition to the mass and energy of the particle, there is a dependence on the fundamental physical Planck's constant h. Planck's constant appears in the Planck hypothesis where it scales the quantum energy of photons, and it appears in atomic energy levels, which are calculated using the Schrödinger equation.

2.3 Calculation of Coulomb Barrier

The height of the Coulomb barrier can be calculated if the nuclear separation and the charges of the particle are known. However, in order to accomplish nuclear fusion, the particles that are involved in this type of thermonuclear reaction must first overcome the electric repulsion Coulomb' force to get close enough for the attractive nuclear strong force to take over to fuse with each other.

This requires extremely high temperatures, if temperature alone is considered in the process and one needs to calculate the temperature required to provide the given energy as an average thermal energy for each particle. Hence, for a gas in thermal equilibrium, which has particles of all velocities, the most probable distribution of these velocities obeys Maxwellian distribution, where we can calculate this thermal energy. In the case of the proton cycle in stars, this barrier is penetrated by tunneling, allowing the process to proceed at lower temperatures than that which would be required at pressures attainable in the laboratory.

Considering the barrier to be the electric potential energy of two point charges (e.g., point), the energy required to reach a separation r is given by the following relation as general form of Eq. 2.1, and it is

$$U = \frac{ke^2}{r} \qquad \text{(Eq. 2.5)}$$

where k is Coulomb's constant and e is the proton charge. Given the radius r at which the nuclear attractive force becomes dominant, the temperature necessary to raise the average thermal energy to that point can be calculated.

The thermal energy is a physical notion of "temperature," which is *average translation kinetic energy* possessed by free particles given by *equipartition of energy*, which is sometimes called the thermal energy per particle. It is useful in making judgments about whether the internal energy possessed by a system of particles will be sufficient to cause other phenomena. It is also useful for comparisons of other types of energy possessed by a particle to that which it possesses simply as a result of its temperature. Additionally, from classical thermodynamics point of view, internal energy is the energy associated with the random disordered motion of molecules. It is separated in scale from the macroscopic ordered energy associated with moving objects; it refers to the invisible microscopic energy on the atomic and molecular scale [2].

Note that the equipartition of energy theorem states that molecules in thermal equilibrium have the same average energy associated with each independent degree of freedom of their motion and that the energy is

$\frac{1}{2}kT$ Per molecule	$k =$ Boltzmann's constant	$\frac{3}{2}kT$
$\frac{1}{2}RT$ Per mole	$R =$ gas constant	$\frac{3}{2}RT$

For three translational degrees of freedom, such as in an ideal mono-atomic gas, the above statements are true, and the equipartition result is then given by

$$\mathrm{KE}_{\mathrm{avg}} = \frac{3}{2}kT \qquad \text{(Eq. 2.6)}$$

Equation 2.6 serves well in the definition of kinetic temperature since that involves just the translational degrees of freedom, but it fails to predict the specific heats of polyatomic gases because the increase in internal energy associated with heating of such gases adds energy to rotational and perhaps vibrational degrees of freedom. Each vibrational mode will get $kT/2$ for kinetic energy and $kT/2$ for potential energy—equality of kinetic and potential energy is addressed in the *virial theorem*. Equipartition of energy also has implication for electromagnetic radiation when it is in equilibrium with matter, each mode of radiation having kT of energy in the Rayleigh-Jeans law.

To prove the result of equipartition theory that is given by Eq. 2.6 and follows the Boltzmann distribution, we do the following analyses. We easily derive this equation, by considering a gas in which the particles can move only in one dimension for the purpose of simplicity of the calculation, and in addition, we

consider a strong magnetic field that can constrain electrons to move only the field lines; thus, the one-dimensional Maxwellian distribution is given by the following formula as

$$f(u) = A\exp\left(-\frac{1}{2}mu^2/kT\right) \qquad \text{(Eq. 2.7)}$$

where $f(u)du$ is the number of particles per m^3 with velocity between u and $u + du$, where $mu^2/2$ is the kinetic energy and k is the Boltzmann constant and its value is equal to 1.38×10^{-23} J/K. The constant A is related to particle density A, as it is shown below

$$A = n\left(\frac{m}{2\pi kT}\right)^{1/2} \qquad \text{(Eq. 2.8)}$$

and this density is analyzed below.

Using Fig. 2.4, we can write the formula for particle density n, or number of particles per m^3, which is given by

$$n = \int_{-\infty}^{+\infty} f(u)du \qquad \text{(Eq. 2.9)}$$

The width of the distribution in Fig. 2.4 is characterized by the constant T, which we call the temperature. To have a concept of the exact meaning of temperature T, we can compute the average kinetic energy of particles within this distribution.

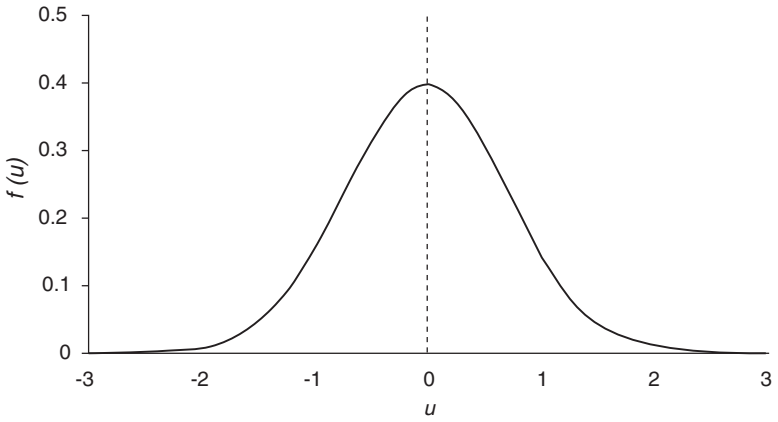

Fig. 2.4 A Maxwellian velocity distribution

$$\mathrm{KE}_{\mathrm{avg}} = \frac{\int_{-\infty}^{+\infty} \frac{1}{2} m u^2 f(u) du}{\int_{-\infty}^{+\infty} f(u) du} \qquad \text{(Eq. 2.10)}$$

A new variable v_{th} is defined as

$$v_{\mathrm{th}} = (2kT/m)^{1/2} \qquad \text{(Eq. 2.11)}$$

Substitution of this new variable results in Eqs. 2.7 and 2.10 to become as

$$\begin{aligned} f(u) &= A \exp\left(-\frac{u^2}{v_{\mathrm{th}}}\right) \\ \mathrm{KE}_{\mathrm{avg}} &= \frac{\frac{1}{2} m A v_{\mathrm{th}}^3 \int_{-\infty}^{+\infty} \left[\exp\left(-y^2\right)\right] y^2 dy}{A v_{\mathrm{th}} \int_{-\infty}^{+\infty} [\exp(-y^2)] dy} \end{aligned} \qquad \text{(Eq. 2.12)}$$

The integral in the numerator, in the second equation set of Eq. 2.12, is integrable by parts as

$$\begin{aligned} \int_{-\infty}^{+\infty} y \cdot [\exp(-y^2)] y dy &= \left\{ -\frac{1}{2} \left[\exp\left(-y^2\right)\right] y \right\}_{-\infty}^{+\infty} - \int_{-\infty}^{+\infty} -\frac{1}{2} \exp\left(-y^2\right) dy \\ &= \frac{1}{2} \int_{-\infty}^{+\infty} \exp\left(-y^2\right) dy = A v_{\mathrm{th}} \end{aligned} \qquad \text{(Eq. 2.13)}$$

Substitution of Eq. 2.13 into Eq. 2.12 and cancelling the common integrals from denominator and numerator result in the following relation for average kinetic energy as

$$\mathrm{KE}_{\mathrm{avg}} = \frac{\frac{1}{2} m A v_{\mathrm{th}}^3 \cdot \frac{1}{2}}{A v_{\mathrm{th}}} = \frac{1}{4} m v_{\mathrm{th}}^2 = \frac{1}{2} kT \qquad \text{(Eq. 2.14)}$$

which is proof of equipartition scenario and indicates that the average kinetic energy is $\frac{1}{2}kT$. By similar analyses, Eq. 2.14 can be easily expanded to three-dimensional form; therefore, the Maxwellian distribution for three-dimensional Cartesian coordinate system becomes

$$f(u, v, w) = A_3 \exp\left[\frac{1}{2}\left(u^2 + v^2 + w^2\right)/kT\right] \qquad \text{(Eq. 2.15)}$$

where constant A_3 is given as

$$A_3 = n\left(\frac{m}{2\pi kT}\right)^{3/2} \quad \text{(Eq. 2.16)}$$

In that case, the average kinetic energy $\mathrm{KE}_{\mathrm{avg}}$ is presented by

$$\mathrm{KE}_{\mathrm{avg}} = \frac{\int\int\int_{-\infty}^{+\infty} (A_3)\frac{1}{2}m\left(u^2+v^2+w^2\right)\exp\left[-\frac{1}{2}\left(u^2+v^2+w^2\right)/kT\right]dudvdw}{\int\int\int_{-\infty}^{+\infty} A_3\exp\left[-\frac{1}{2}\left(u^2+v^2+w^2\right)/kT\right]dudvdw} \quad \text{(Eq. 2.17)}$$

Equation 2.17 is symmetric in variables u, v, and w, since a Maxwellian distribution is isotropic. As result, each of three terms in the numerator is the same as the others; hence all we need to do is to evaluate the first and multiply it by three and get the following result as

$$\mathrm{KE}_{\mathrm{ave}} = \frac{3A_3\int\frac{1}{2}mu^2\exp\left(-\frac{1}{2}mu^2/kT\right)du\int\int\exp\left[-\frac{1}{2}m\left(v^2+w^2\right)/kT\right]dvdw}{A_3\int\exp\left(-\frac{1}{2}mu^2/kT\right)du\int\int\exp\left[-\frac{1}{2}m\left(v^2+w^2\right)/kT\right]dvdw} \quad \text{(Eq. 2.18)}$$

Using our previous result, we have

$$\mathrm{KE}_{\mathrm{ave}} = \frac{3}{2}kT \quad \text{(Eq. 2.19)}$$

The result of Eq. 2.19 and mathematical process of obtaining it is proof of Eq. 2.6, which we stated above, and it is an indication of $\mathrm{KE}_{\mathrm{ave}}$ in general which is equals to $\frac{1}{2}kT$ per degree of freedom.

Since temperature T and average kinetic energy $\mathrm{KE}_{\mathrm{ave}}$ are so closely related, it is customary in plasma physics to give temperatures in units of energy. To avoid confusion on the number of dimensions involved, it is not $\mathrm{KE}_{\mathrm{ave}}$ but the energy corresponding to kT that is used to denote the temperature. For $kT = 1\ \mathrm{eV} = 1.6 \times 10^{-19}\ \mathrm{J}$, we have

$$T = \frac{1.6 \times 10^{-19}}{1.38 \times 10^{-23}} = 11,600 \quad \text{(Eq. 2.20)}$$

Thus, the conversion factor is

$$1\mathrm{eV} = 11,600\,\mathrm{K}$$

2.4 Thermonuclear Fusion Reactions

As part of thermonuclear fusion reaction system, we have to have some understanding of energies related to the reacting nuclei that are following a Maxwellian distribution and the problem in hand, and this distribution can be presented by

$$dn = \text{constant} \times \frac{E^{1/2}}{T^{13/2}} \exp\left(-\frac{E}{kT}\right) dE \qquad \text{(Eq. 2.21)}$$

where dn is the number of nuclei per unit volume whose energies, in the frame of the system, lie in the range from E to $E + dE$, k is again Boltzmann constant and is equal to 1.38×10^{-16} erg/K, and T is the *kinetic temperature*. The definition of kinetic temperature of a system of particles falls in the fact that the temperature appropriate to Maxwellian distribution is assumed by the particles upon equipartition of energy among the three translational degrees of freedom. The mean particle energy is then $3kT/2$ as it was defined by Eq. 2.19.

Incidentally, when a system is in blackbody radiation equilibrium, per description given by Glasstone and Lovberg [1], the radiation pressure is equal to $\alpha T^4/c$, where c is the velocity of light. For a temperature of 10 keV, i.e., 1.16×10^8 K, this would be the order of 10^{11} atm. In stars, such high pressures are balanced by gravitational forces due to the enormous masses. Naturally, there exists no practical controlled thermonuclear reactor that could withstand the pressure resulting from the equilibrium with radiation at extremely high temperature. Thus, the solution around this problem is by utilization of the very low particle densities required by other considerations. A system of this type is optically "thin" and transparent to essentially all the Bremsstrahlung emission from a hot plasma; it is a poor absorber, and hence also a poor emitter, of this radiation. The radiation field with which the particles may be in equilibrium is then very much weaker than blackbody radiation. In other words, the equivalent radiation temperature is much lower than kinetic temperature, which is related to the energy distribution among the particles [1].

It is for this reason that the term kinetic temperature, rather than just temperature without qualification, has been frequently used in the preceding text. Strictly speaking, "temperature" implies thermodynamic equilibrium, which means both kinetic and blackbody radiation equilibrium [2].

Theoretically it has been proved that the energy of the interacting particles presented by the atomic numbers by Z_1 and Z_2, with individual mass m_1 and m_2, is well below the top of the Coulomb barrier. In addition, the cross section for the combination of two nuclei can be written down to a good approximation in the form of Eq. 2.22, as a function of the relative particle energy E, which represents the total kinetic energy of the two nuclei in the center-of-mass system as

$$\sigma(E) \approx \frac{\text{Constant}}{E^{3/2}} \cdot \exp\left[-\frac{2^{3/2}\pi^2 M^{1/2} Z_1 Z_2 e^2}{hE^{1/2}}\right] \qquad \text{(Eq. 2.22)}$$

where h is the Planck constant and M is the reduced mass of two individual particles interacting with each other and expressed as

$$M = \frac{m_1 m_2}{m_1 + m_2} \qquad \text{(Eq. 2.23)}$$

In addition, Eq. 2.22 revels that the fusion reaction has a finite cross section, even when the relative energy of the nuclei is quite small; however, because the exponential term in that equation is the dominating factor, the cross section increases rapidly as the relative particle energy increases. It can be noted as well that for a given value of the relative energy, the reaction cross section decreases with increasing atomic number of the interacting nuclei [1].

Now to investigate the contribution to the overall reaction rate per unit energy interval made by nuclei with relative energy in the range from K to $E + dE$ in a thermonuclear system, at the kinetic temperature T, it is proportional to the product of $\sigma(E)$ and of dn/dE for that particular temperature. This contribution may be expressed by $R(E)$, so that, from Eqs. 2.21 and 2.22,

$$R(E) \approx \frac{C}{E^{3/2}T^{3/2}} \exp\left[-\frac{2^{3/2}\pi^2 M^{1/2} Z_1 Z_2 e^2}{hE^{1/2}} - \frac{E}{kT}\right] \qquad \text{(Eq. 2.24)}$$

where C is a constant [1].

Figure 2.5 shows the significance of Eq. 2.24 here, and the curve marked dn/dE is an atypical Maxwellian distribution of the relative particle energies for a specified kinetic temperature.

The cross section variation for the nuclear fusion reaction with the relative energy, as determined by Eq. 2.22, is shown by curve $\sigma(E)$. The dependence of the contribution to the reaction rate made by particles of relative energy E, obtained by multiplying the ordinates of the other two curves, is indicated by the curve in the center of Fig. 2.5. It can be seen that this curve has a distinct maximum corresponding to the relative energy E_m, so that nuclei having this amount of relative energy make the maximum contribution to the total fusion reaction rate [1].

The average energy of the nuclei is in the vicinity of the maximum of the dn/dE curve; therefore, it is evident that E_m is larger than the average energy for the given kinetic temperature.

Hence, in order to determine the total reaction, we need to determine the total area under the curve of $\sigma(E)dn/dE$ in Fig. 2.5 by integrating over the function curve $\sigma(E)dn/dE$, from energy point 1 to point 2. Consequently, it is obvious most of the considered thermonuclear reaction will be due to a relatively small fraction of the nuclear collisions in which the relative energies are greatly in excess of the average.

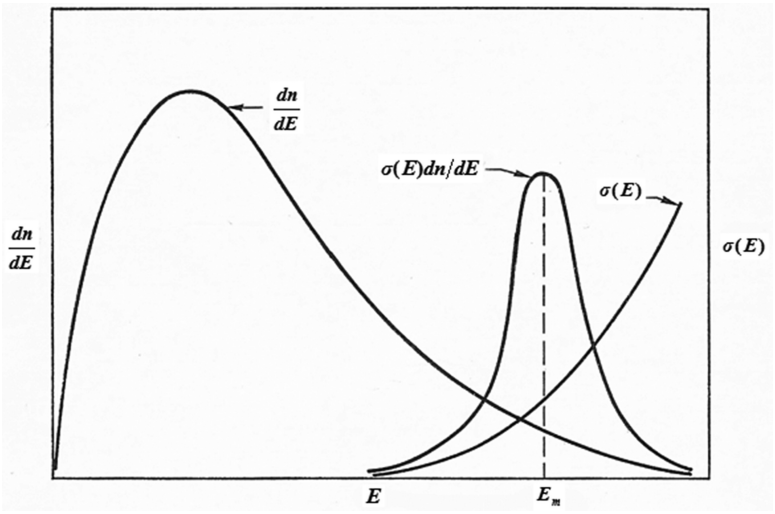

Fig. 2.5 Effect of Maxwellian energy distribution on nuclear reaction rate

The preceding text explains why there is an advantage in performing a nuclear fusion reaction, e.g., with uniformly accelerated particles, to permit the nuclei to become "thermalized," that is, to attain a Maxwellian distribution of energies, as a result of collision.

Now, we can calculate the maximum relative energy E_m, by differentiation in Eq. 2.24 in respect to energy E_m, provided that the kinetic temperature is not too high. However, the variation E_m with E_m is determined almost entirely by the exponential factor in Eq. 2.24; hence, a good approximation to the value of E_m in Fig. 2.5 can be obtained by calculating the energy for which this factor is a maximum, and this value is found to be

$$E_m \approx \left[\frac{(2M)^{1/2}\pi^2 Z_1 Z_2 e^2 kT}{h}\right]^{2/3} \qquad \text{(Eq. 2.25)}$$

The expression in Eq. 2.25 gives the relative energy in nuclear collision making the maximum contribution to the reaction rate at the not too highly kinetic temperature T. Dividing both sides of Eq. 2.25 by kT, we obtain the following result as

$$\frac{E_m}{kT} \approx \left[\frac{(2M)^{1/2}\pi^2 Z_1 Z_2 e^2}{h}\right]^{2/3} \frac{1}{(kT)^{1/3}} \qquad \text{(Eq. 2.26)}$$

Note that it is a common practice in thermonuclear studies to express kinetic temperature in terms of the corresponding energy kT in kilo-electron volts, i.e., in keV units. Since the Boltzmann constant k is 1.38×10^{-16} erg/K and 1 keV is equivalent to 1.60×10^{-9} erg, it follows that [1]

$$k = 8.6 \times 10^{-8}\,\text{keV}/^{0}\text{K}$$

or

$$1\ \text{keV} = 1.16 \times 10^{7}\,^{0}\text{K}$$

Thus, a temperature of T keV is equivalent to $1.16 \times 10^{7}\ T\ ^{0}$K.

2.5 Rates of Thermonuclear Reactions

Among all the related text to this particular subject that I have personally seen, the best book that describes the rates of thermonuclear reactions is given by Glasstone and Lovberg [1]; consequently, I will use exactly what they have describe for this matter.

Consider a binary reaction in a system containing n_1 nuclei/cm^3 of one reacting element and n_2 of the other. To determine the rate at which the two nuclear elements interact, it may be supposed that the nuclei of the first element kind form a stationary lattice within the nuclei of the second kind which moves at random with a constant velocity υ cm/s, which is equal to the relative velocity of the nuclei. The total cross section for all the stationary nuclei in 1 cm^3 is then $n_1\sigma$ nuclei/cm. This gives the number of nuclei of the first kind with which each nucleus of the second kind will react while traveling a distance of 1 cm. The total distance traversed in 1 s by all the nuclei of the latter type present in 1 cm^3 is equal to $n_2\upsilon$ nuclei/(cm^2 s). Hence, the nuclear reaction rate R_{12} is equal to the product of $n_1\upsilon$ and $n_2\upsilon$; thus

$$R_{12} = n_1 n_2 \sigma \upsilon \quad \text{interaction}/\left(\text{cm}^2\,\text{s}\right) \qquad \text{(Eq. 2.27)}$$

If the reaction occurs between two nuclei of the same kind, e.g., two deuterons, so that n_1 and n_2 are equal, the expression for the nuclear reaction rate, represented by R_{11}, becomes

$$R_{11} = \frac{1}{2} n^2 \sigma \upsilon \quad \text{interaction}/\left(\text{cm}^2\,\text{s}\right) \qquad \text{(Eq. 2.28)}$$

where n is the number of reactant nuclei/cm^3. See Fig. 2.6.

In order that each interaction between identical nuclei is not going to be counted twice, the factor of 1/2 is introduced into Eq. 2.28.

Going forward, the two established Eqs. 2.27 and 2.28 are applicable when the relative velocity of the interacting nuclei is constant, as is true, approximately at least, for high-energy particle from an accelerator. However, for thermonuclear reaction, there would be a distribution of velocities and energies as well, over a wide range.

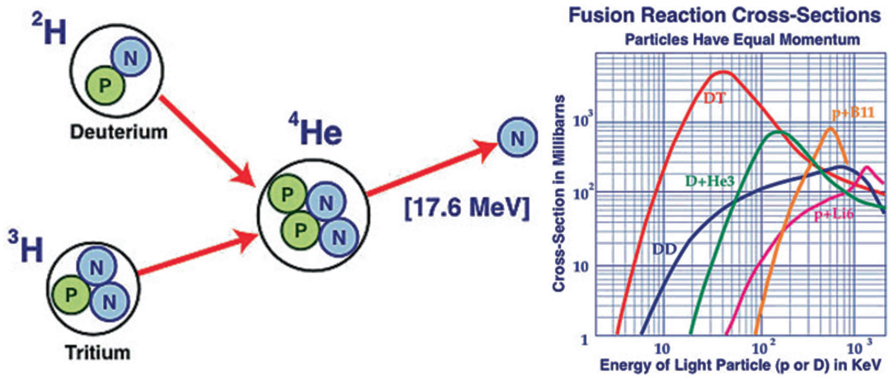

Fig. 2.6 Depiction of all isotope hydrogen thermonuclear reactions

As it is depicted in Fig. 2.6 on the right-hand side, it shows that the reaction cross section is dependent on the energy or velocity, and generally speaking it follows the product $\sigma\upsilon$ in Eqs. 2.27 and 2.28 which needs to be replaced by a value such as the symbol of $\overline{\sigma\upsilon}$, which is averaged over the whole range of relative velocities. Thus, Eq. 2.27 is written as

$$R_{12} = n_1 n_2 \overline{\sigma\upsilon} \quad \text{interaction}/\left(\text{cm}^2\,\text{s}\right) \qquad \text{(Eq. 2.29)}$$

Accordingly, Eq. 2.28 becomes

$$R_{11} = \frac{1}{2} n^2 \overline{\sigma\upsilon} \qquad \text{(Eq. 2.30)}$$

Using reduced mass M expressed by Eq. 2.23, which is the result of the interaction between two individual masses of two elements, can describe the new form of Eq. 2.21, provided that the velocity distribution is Maxwellian and we know that the kinetic energy is $E = M\upsilon^2/2$. Thus, we can write

$$dn = n\left(\frac{M}{2\pi kT}\right)^{3/2} \exp\left(-\frac{M\upsilon^2}{2kT}\right)\upsilon^2 d\upsilon \qquad \text{(Eq. 2.31)}$$

where dn is the number of particles whose velocities relative to that of a given particle lie in the range from υ to $\upsilon + d\upsilon$. Hence, it follows that

$$\overline{\sigma\upsilon} = \frac{\int_0^\infty \sigma\upsilon dn}{\int_0^\infty dn} = \frac{\int_0^\infty \sigma\upsilon\left[\exp\left(-\frac{M\upsilon^2}{2kT}\right)\upsilon^2 d\upsilon\right]}{\int_0^\infty \exp\left(-\frac{M\upsilon^2}{2kT}\right)\upsilon^2 d\upsilon} \qquad \text{(Eq. 2.32)}$$

The integral in the denominator of Eq. 2.32 is equal to $[(2kT/M)^{3/2}](\pi^{1/2}/4)$, and so this equation becomes

$$\overline{\sigma v} = \frac{4}{\pi^{1/2}} \left(\frac{Mv^2}{2kT}\right) \int_0^\infty \sigma \exp\left(-\frac{Mv^2}{2kT}\right) v^2 dv \qquad \text{(Eq. 2.33)}$$

The integral term in Eq. 2.33 can be evaluated by changing the variable. Since nuclear cross sections are always determined and expressed as a function of the energy of the bombarding particle, the bombarded particle being essentially at rest in the target, the actual velocity of the bombarding nucleus is also its relative velocity. Hence, if E is the actual energy, in the laboratory system, of the bombarding nucleus of mass m, then E is written as

$$E = \frac{1}{2} m v^2 \qquad \text{(Eq. 2.34a)}$$

so that

$$v = \left(\frac{2E}{m}\right)^{1/2} \qquad \text{(Eq. 2.34b)}$$

And differentiating both sides of Eq. 2.34b, we get

$$v^2 dv = \frac{2E}{m^2} dE \qquad \text{(Eq. 2.34c)}$$

Substitution of Eq. 2.34c into Eq. 2.33 yields

$$\overline{\sigma v} = \frac{4}{\pi^{1/2}} \left(\frac{M}{2kT}\right)^{3/2} \frac{1}{m^2} \int_0^\infty \sigma \exp\left(-\frac{ME}{mkT}\right) E dE \qquad \text{(Eq. 2.35)}$$

where σ in the integrand is the cross section for a bombarding nucleus of mass m and energy E.

If the temperature T in Eq. 2.35 is expressed in kilo-electron volts, and the values of E are in the same units, it is convenient to rewrite Eq. 2.35 in the new form as

$$\overline{\sigma v} = \left(\frac{8}{\pi^{1/2}}\right)^{1/2} \frac{M^{3/2}}{m^2} \int_0^\infty \sigma \exp\left(-\frac{ME}{mT}\right) \frac{E}{T} dE \qquad \text{(Eq. 2.36)}$$

where the quantity E/T is dimensionless. If σ, determined experimentally, can be expressed as a relatively simple function of E, as is sometimes the case, the integration in Eq. 2.36 may be performed analytically. Alternatively, numerical methods, for example, Simpson's rule, may be employed.

In any event, the values of $\overline{\sigma v}$ for various kinetic temperatures can be derived from Eq. 2.36, based on a Maxwellian distribution of energies or velocities, and the results can be inserted in Eq. 2.29 or Eq. 2.30 to give the rate of a thermonuclear reaction at a specified temperature.

2.6 Thermonuclear Fusion Reactions

In a thermonuclear fusion reaction, two light nuclear masses are forced together, and then they will fuse with a yield of energy as it is depicted in Fig. 2.7. The reason behind the energy yield is due to the fact that the mass of the combination of fusion reaction will be less than the sum of the masses of the individual nuclei.

If the combined nuclear mass is less than that of iron at the peak of the binding energy curve, then the nuclear particles will be more tightly bound than they were in the lighter nuclei, and that decrease in mass comes off in the form of energy according to the Einstein relationship. However, for elements heavier than iron, fission reaction will yield energy.

The Einstein relationship that is known as theory of relativity indicates that relativistic energy is presented as

$$E = mc^2 \qquad \text{(Eq. 2.37)}$$

where m is an effective relativistic mass of particle traveling at a very high of speed c. Equation including both the kinetic energy and rest mass energy m_0 for a particle can be calculated from the following relation.

$$\text{KE} = mc^2 - m_0c^2 \qquad \text{(Eq. 2.38)}$$

Further analysis of Einstein relativity theory allows us to blend into Eq. 2.38, the relativistic momentum p expression as

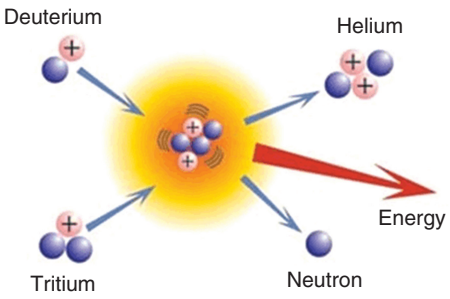

Fig. 2.7 A thermonuclear fusion reaction

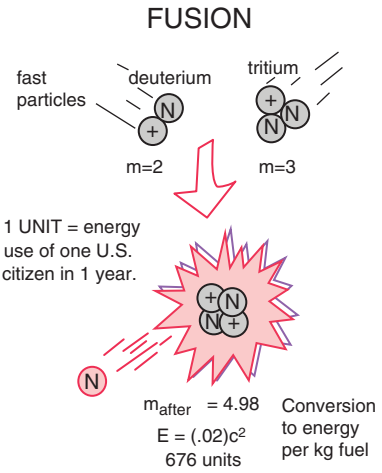

Fig. 2.8 Deuterium-tritium fusion reaction

$$p = \frac{m_0 v}{\sqrt{1 - \frac{v^2}{c^2}}} \qquad \text{(Eq. 2.39)}$$

The combination relativistic momentum p and particle speed c show up often in relativistic quantum mechanics and relativistic mechanics as multiplication of pc, and it can be manipulated as follows, using conceptual illustration such as Fig. 2.8:

$$p^2c^2 = \frac{m_0^2 v^2 c^2}{1 - \frac{v^2}{c^2}} = \frac{m_0^2 \frac{v^2}{c^2} c^4}{1 - \frac{v^2}{c^2}} \qquad \text{(Eq. 2.40a)}$$

and by adding and subtracting a term, it can be put in the form:

$$p^2c^2 = \frac{m_0^2 c^4 \left[\frac{v^2}{c^2} - 1\right]}{1 - \frac{v^2}{c^2}} + \frac{m_0^2 c^4}{1 - \frac{v^2}{c^2}} = -m_0^2 c^4 + \left(mc^2\right)^2 \qquad \text{(Eq. 2.40b)}$$

which may be rearranged to give the following expression for energy:

$$E = \sqrt{p^2c^2 + \left(m_0 c^2\right)^2} \qquad \text{(Eq. 2.40c)}$$

Note that again the m_0 is the rest mass and m is the effective relativistic mass of particle of interest at very high speed c.

Per Eq. 2.40c, the relativistic energy of a particle can also be expressed in terms of its momentum in the expression such as

$$E = mc^2 = \sqrt{p^2c^2 + m_0^2c^4} \qquad \text{(Eq. 2.41)}$$

The relativistic energy expression is the tool used to calculate binding energies of nuclei and energy yields of both nuclear fission and thermonuclear fusion reactions.

Bear in your mind that the nuclear binding energy is rising from the fact that nuclei are made up of proton and neutron, but the mass of a nucleus is always less than the sum of the individual masses of the protons and neutrons, which constitute it. The difference is a measure of the nuclear binding energy, which holds the nucleus together. This binding energy can be calculated from the Einstein relationship:

$$\text{Nuclear binding energy} = \Delta mc^2 \qquad \text{(Eq. 2.42)}$$

Now that we have better understanding of physics of thermonuclear fusion reaction and we explained what the Coulomb berries and energy is all about, we pay our attention to thermonuclear fusion reaction of hydrogen, which is fundamental chemical element of generating energy-driven controlled fusion.

According to Glasstone and Lovberg [1], "because of the increased height of the Coulomb energy barrier with increasing atomic number, it is generally true that, at a given temperature, reactions involving the nuclei of hydrogen isotopes take place more readily than do analogous reactions with heavier nuclei. In view of the greater abundance of the lightest isotope of the hydrogen, with mass number 1, it is natural to see if thermonuclear fusion reactions involving this isotope could be used for the release of energy" [1].

Unfortunately, the three possible reactions between hydrogen (H) nuclei alone or with deuterium (D) or tritium (T) nuclei, i.e.,

$$\begin{aligned} {}_1\mathrm{H}^1 + {}_1\mathrm{H}^1 &\rightarrow {}_1\mathrm{D}^2 + {}_1\mathrm{e}^0 \\ {}_1\mathrm{H}^1 + {}_1\mathrm{D}^2 &\rightarrow {}_1\mathrm{D}^2 + \gamma \\ {}_1\mathrm{H}^1 + {}_1\mathrm{T}^3 &\rightarrow {}_2\mathrm{He}^4 + \gamma \end{aligned}$$

are known to have cross sections that are too small to permit a net gain of energy at temperature, which may be regarded as attainable [1].

Consequently, recourse must have to be the next most abundant isotope, i.e., deuterium, and here two reactions, which occur at approximately the same rate over a considerable range of energies, are of interest; these are the D-D reactions as

$${}_1\mathrm{D}^2 + {}_1\mathrm{D}^2 \rightarrow {}_2\mathrm{He}^3 + {}_1\mathrm{n}^0 + 3.27\,\mathrm{MeV}$$

and

$$_1D^2 + _1D^2 \rightarrow {}_2T^3 + {}_1H^0 + 4.03\,\text{MeV}$$

called the "neutron branch" and the "proton branch," respectively. The tritium produced in the proton branch or obtained in another way, as explained below, can then react, at a considerably faster rate, with deuterium nuclei in the D-T reaction as

$$_1D^2 + _1T^3 \rightarrow {}_2He^4 + {}_1n^0 + 17.60\,\text{MeV}$$

The He^3 formed in the first D-D reaction can also react with deuterium; thus,

$$_1D^2 + _1He^3 \rightarrow {}_2He^4 + {}_1H^0 + 18.30\,\text{MeV}$$

This reaction is of interest because, as in the D-T reaction, there is a large energy release; the D-He^3 reaction is, however, slower than the other at low thermonuclear temperatures, but its rate approached that of the D-D reactions at 100 keV and is demonstrated in Fig. 2.9.

In the methods of currently under consideration for production of thermonuclear power, the fast neutrons produced in neutron branch of the D-D reactions and in the D-T reactions would most probably escape from the immediate reaction environment. Thus, considering a suitable moderator to slow down these neutrons which is either water, lithium, or beryllium, with the liberation of their kinetic energy in form of heat, can be utilized.

$$_3Li^6 + {}_0n^1 \rightarrow {}_2He^4 + {}_1T^3 + 4.6\,\text{MeV}$$

The slow neutrons can then be captured in lithium-6, which constitutes 7.5 at.% of natural lithium, by the reaction in above, leading to the production of tritium. The energy released can be used as heat, and the tritium can, in principle, be transferred to the thermonuclear system to react with deuterium.

If we produce enough initial ignition temperature to the above four thermonuclear reactions, all four fusion processes will take place, and the two neutrons produced would subsequently be captured by lithium-6.

By means of the quantum mechanics theory of Coulomb barrier penetration, it is much more convenient to make use of cross sections obtained experimentally as it is plotted in Fig. 2.9 for reactions such as D-D, D-T, and D-He^3, by bombarding targets containing deuterium, tritium, or helium-3 with deuterons of known energies. Technically, for the purpose of marginal safety measurements of the cross section, it is normally done with order-of-magnitude estimation, at least, of the rates or cross section of thermonuclear reactions obtained experimentally.

It will be observed that the D-T curve demonstrates a maximum at energy of 110 keV, which is an example of the resonance phenomenon, which often occurs in nuclear reactions [1].

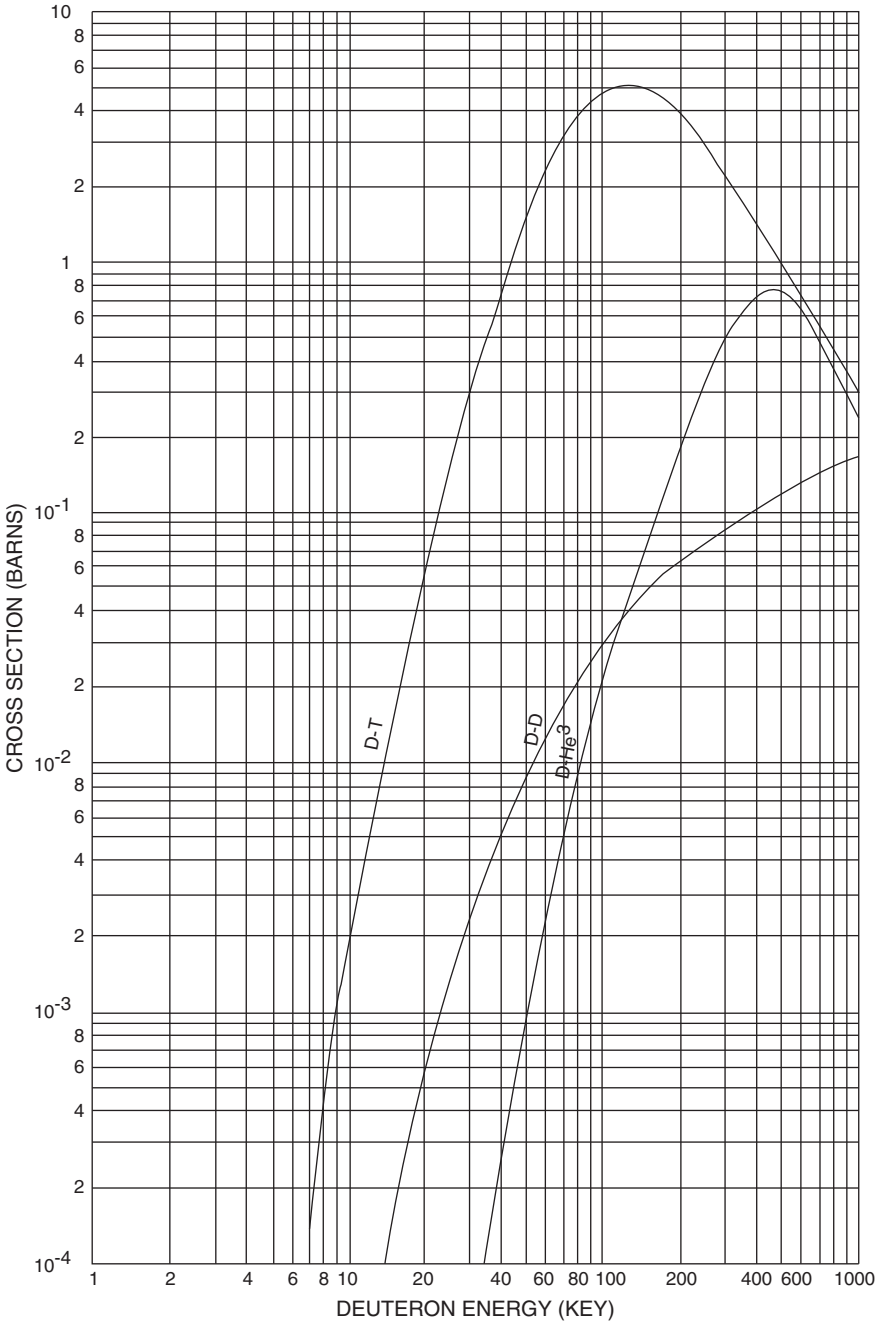

Fig. 2.9 Cross sections for D-T, D-D total, and D-He^3 reactions

However, the appreciable cross sections for energies well below the top of the Coulomb barriers for each of the reaction studies provide an experimental illustration of the reality of the barrier penetration effect.

The data in Fig. 2.9, for particular deuteron energies, are applied to the determination of the average $\overline{\sigma v}$, that is, presented by Eqs. 2.35 and 2.36, assuming a Maxwellian distribution of particle energies or velocities. Figure 2.10 here shows the result of integration presented by Eq. 2.36 and the curve that gives $\overline{\sigma v}$ in cm^3/s as a function of the kinetic temperature of the reaction system in kilo-electron volts. The values in plot Fig. 2.10 for a number of temperatures are also marked in Table 2.1 here.

In Figs. 2.9 and 2.10, they both illustrate the overall effect on the thermonuclear fusion reaction rates that are taking into account the Maxwellian distribution.

Analytical expression for σ and $\overline{\sigma v}$ for the D-D and D-T fusion reactions can be obtained by utilizing Eq. 2.24 in a somewhat modified form. The relative kinetic energy E of the nuclei is given as

$$E = \frac{1}{2} M v^2 \qquad \text{(Eq. 2.43)}$$

where v is the relative velocity and the deuteron energy E_D, in terms of which the cross section is expressed, is $m_\mathrm{D} v^2/2$, where m_D is the mass of the deuteron. Hence, $(M/E)^{1/2}$ in Eq. 2.24 may be replaced by $(m_\mathrm{D}/E_\mathrm{D})^{1/2}$; since Z_1 and Z_2 are both unity, the result then is

$$\begin{aligned} \sigma(E_\mathrm{D}) &= \frac{C}{E_\mathrm{D}} \exp\left[-\frac{2^{3/2} \pi^2 {m_\mathrm{D}}^{1/2} e^2}{h E_\mathrm{D}^{1/2}} \right] \\ &= \frac{C}{E_\mathrm{D}} \exp\left[-\frac{44.24}{E_\mathrm{D}^{1/2}} \right] \end{aligned} \qquad \text{(Eq. 2.44)}$$

with E_D is expressed in kilo-electron volts. Note that the potential factor is the same for both D-D and D-T thermonuclear fusion reactions, with the deuteron as the projectile particle. The factor preceding the exponential will, however, be different in the two cases [1].

Now if we are interested in mean free path reaction λ, in a system containing n nuclei/cm^3 of a particular reacting species, then λ is the average distance traveled by a nucleus before it undergoes reaction, which is equal to $1/n\sigma$, where σ is the cross section for the given reaction [1].

We replace σ with $\overline{\sigma}$, if we take a Maxwellian distribution which is considered, and in this case the averaged cross section $\overline{\sigma}$ is taken over all energies from zero to infinity, at a given kinetic temperature.

Figure 2.11 is the illustration of the mean free path values for a deuteron in centimeter as a function of the deuteron particle density n, in nuclei/cm^3, for the D-D and D-T reactions at two kinetic temperatures, 10 and 100 keV, in each case

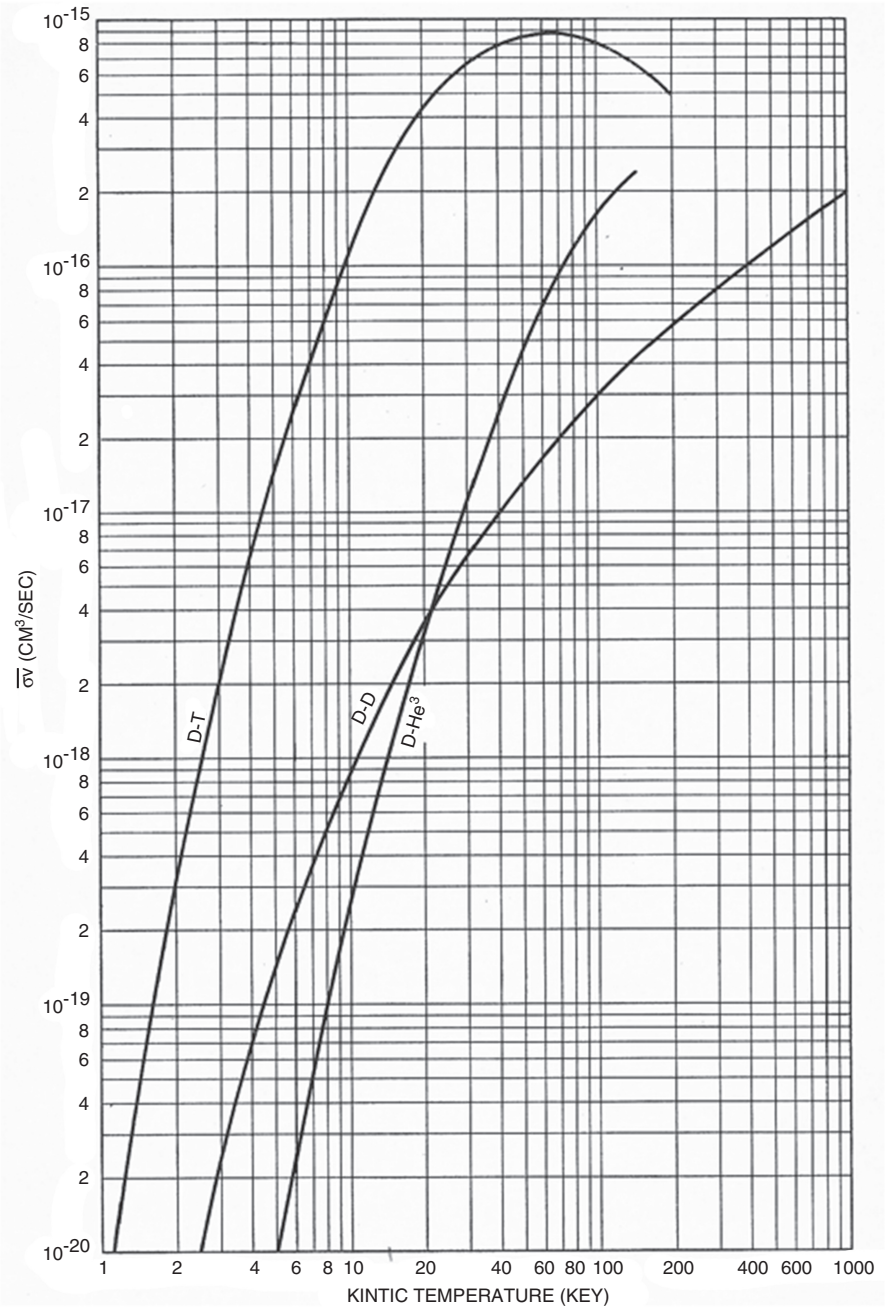

Fig. 2.10 Values of $\overline{\sigma v}$ based on Maxwellian distribution for D-T, D-D (total), and D-He^3 reactions

Table 2.1 Values of $\overline{\sigma v}$ at specified kinetic temperature

Temperature (keV)	D-D (cm^3/s)	D-T (cm^3/s)	D-He^3 (cm^3/s)
1.0	2×10^{-22}	7×10^{-21}	6×10^{-28}
2.0	5×10^{-21}	3×10^{-19}	2×10^{-23}
5.0	1.5×10^{-19}	1.4×10^{-17}	1×10^{-20}
10.0	8.6×10^{-19}	1.1×10^{-16}	2.4×10^{-19}
20.0	3.6×10^{-18}	4.3×10^{-16}	3.2×10^{-19}
60.0	1.6×10^{-17}	8.7×10^{-16}	7×10^{-17}
100.0	3.0×10^{-17}	8.1×10^{-16}	1.7×10^{-18}

and temperatures of these orders of magnitude would be required in a controlled thermonuclear fusion reactor.

The particle of interest for possible fusion reaction for controlled thermonuclear process has possible density of about 10^{15} deuterons/cm^3, and the mean free path at 100 keV for the D-D reaction, according to Fig. 2.11, is about 2×10^{16} cm. This statement translates to the fact that, at the specified temperature and particle density, a deuteron would travel on the average, a distance of 120,000 miles before reacting. For D-T reaction, the mean free paths are shorter, because of the large cross sections for deuterons of given energies, but they are still large in comparison with the dimensions of normal equipment. All of these results play a great deal of impotency to the problem of confinement of the particles in a thermonuclear fusion reacting system such as tokamak machine or any other means.

For the purpose of obtaining a power density P_{DD} of thermonuclear fusion reaction, such as D-D, we use either Eq. 2.29 or Eq. 2.30, to calculate the rate of thermonuclear energy production. If we assume an amount of average energy Q in erg is produced per nuclear interaction, then using Eq. 2.30, it follows that

$$\text{Rate of energy release} = \frac{1}{2} n_D^2 \overline{\sigma v} Q \ \text{ergs}/\left(\text{cm}^3\,\text{s}\right) \qquad \text{(Eq. 2.45)}$$

If the dimension of power density P_{DD} is given in Watts/cm^3, which is equal to 10^7 ergs/(cm^3 s), then we can write

$$P_{DD} = \frac{1}{2} n_D^2 \overline{\sigma v} Q \times 10^{-7} \qquad \text{(Eq. 2.46)}$$

with n_D in deuterons/cm^3, $\overline{\sigma v}$ in units of cm^3/s, and average energy Q in erg.

For every two D-D interactions, an average of 8.3 MeV of energy is deposited within the reacting system. The energy Q per interaction is thus $(1/2) \times 8.3 \times 1.60 \times 10^{-6} = 6.6 \times 10^{-6}$ erg, and upon substitution into Eq. 2.46, it yields that

$$P_{DD} = 3.3 \times 10^{-13} n_D^2 \overline{\sigma v} \ \text{W/cm}^3 \qquad \text{(Eq. 2.47)}$$

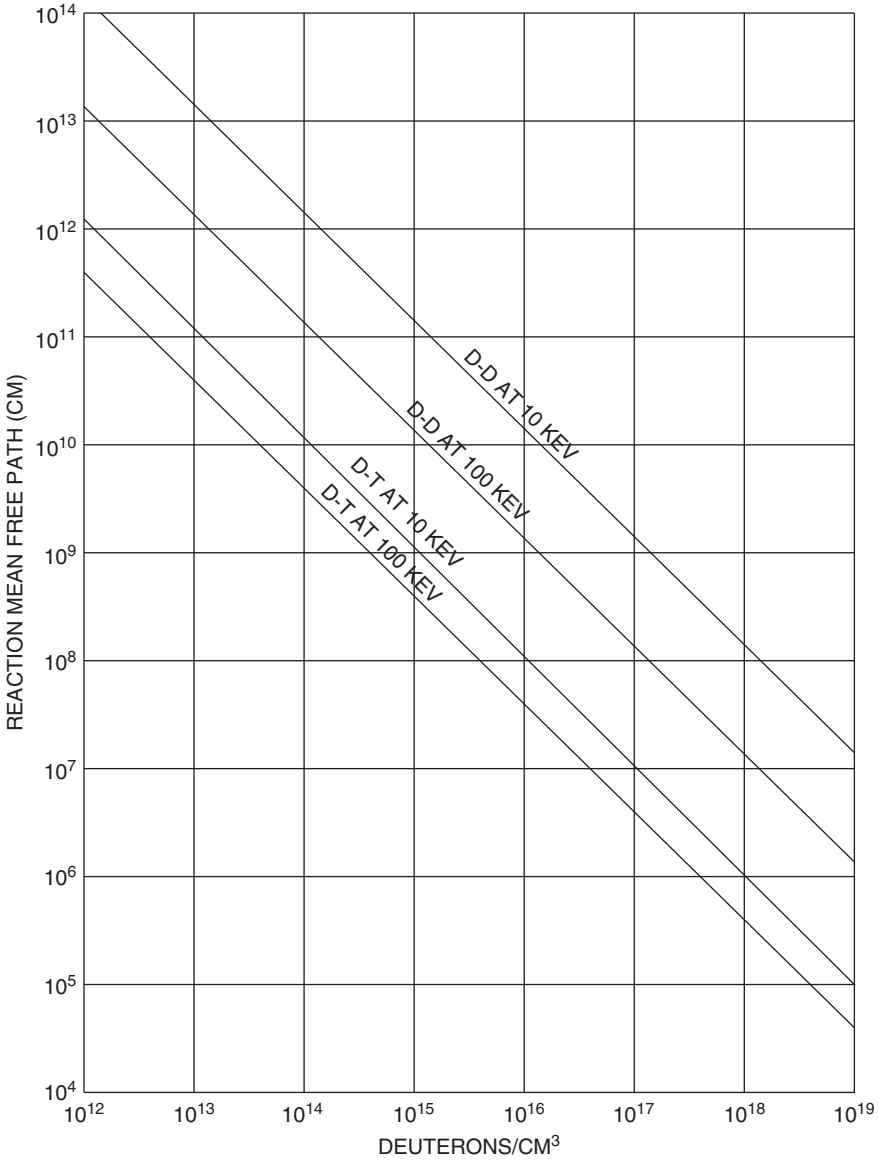

Fig. 2.11 Mean free path for D-T and D-D (total) thermonuclear reactions

As an example for utilization of Eq. 2.46, we look at a D-D reaction at 10 keV, and from Fig. 2.10 or Table 2.1, for given kinetic temperature, we see that $\overline{\sigma v}$ is equal to 8.6×10^{-19} cm^3/s; therefore, the power density is

$$P_{\mathrm{DD}}(10\,\mathrm{keV}) = 2.8 \times 10^{-31} n_{\mathrm{D}}^2 \ \mathrm{W/cm^3} \qquad \text{(Eq. 2.48)}$$

and at 100 keV, when $\overline{\sigma v}$ is equal 3.0×10^{-17} cm^3/s, the power density will be

$$P_{DD}(100\,\text{keV}) = 10^{-29} n_D^2 \text{ W/cm}^3 \quad \text{(Eq. 2.49)}$$

Similar analysis can be performed for thermonuclear reaction fusion reaction of D-T, knowing that the energy remaining in the system per interaction is 3.5 MeV, i.e., $3.5 \times 1.6 \times 10^{-6}$ erg, then the reaction rate is given by Eq. 2.29, and therefore, the thermonuclear reactor density power is

$$P_{DT} = \frac{1}{2} n_D n_T \overline{\sigma v} Q \times 10^{-7} \quad \text{(Eq. 2.50)}$$

where in this case, the average energy Q is 5.6×10^{-6} erg, hence,

$$P_{DT}(10\,\text{keV}) = 6.2 \times 10^{-13} n_D n_T \text{ W/cm}^3 \quad \text{(Eq. 2.51)}$$

and

$$P_{DT}(100\,\text{keV}) = 4.5 \times 10^{-28} n_D n_T \text{ W/cm}^3 \quad \text{(Eq. 2.52)}$$

There is no exact parallel correlation between the conditions of heat transfer and operating pressures, which limit the power density of a fission reactor and those which might apply to a thermonuclear fusion reactor. Nevertheless, there must be similar limitations upon power transfer in a continuously operating thermonuclear reactor as in other electrical power systems.

A large steam-powered electrical generating plant has a power of about 500 MW, i.e., 5×10^8 W. Figure 2.12 is illustrating that 100 keV in a D-D reactor has a power of 5×10^8 W which would provide a reacting volume of only 0.03 cm^3 with deuteron particle densities equivalent to those at standard temperature.

Meanwhile, the gas kinetic pressure exerted by the thermonuclear fuel would be about 10^7 atm or 1.5×10^8 psi. Since the mean reaction lifetime is only a few milliseconds under the conditions specified, it is obvious that the situation would be completely impractical [1].

From what have been discussed so far, it seems that the particle density in a practical thermonuclear reactor must be near 10^{15} nuclei/cm^3. Other problems are associated with the controlled thermonuclear fusion reaction for plasma confinement, and that is why the density cannot be much larger, and it can be explained via stability requirements that are frequently restricted by dimensionless ration β. This ratio is defined as part of convenience in plasma confinement driven by magnetic field, which is equal to the kinetic pressure of the particles in plasma in terms of its ration to the external magnetic pressure or energy density, which is defined by Eq. 3.85 in Chap. 3 of this book.

Details of this dimensionless parameter will be defined toward the end of this chapter as well.

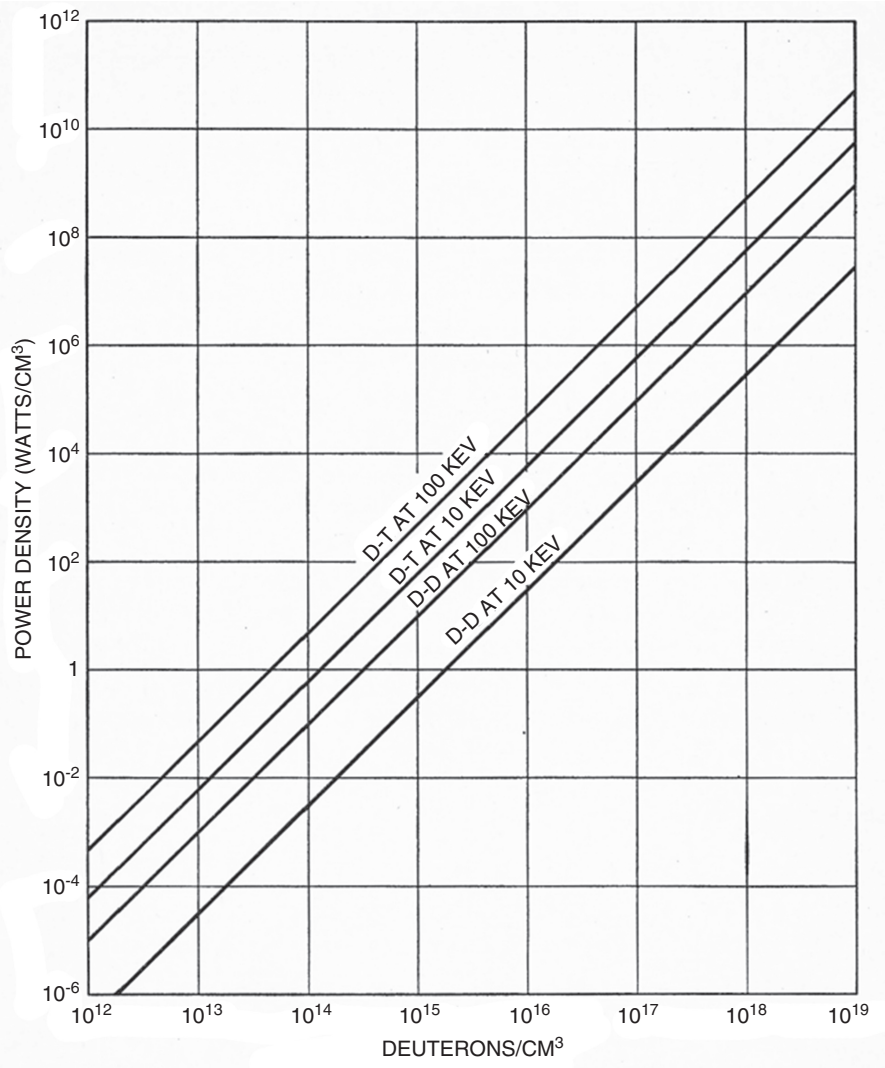

Fig. 2.12 Power densities for D-T and D-D (total) thermonuclear reactions

2.7 Critical Ignition Temperature for Fusion

The fusion temperature obtained by setting the average thermal energy equal to the coulomb barrier gives too high a temperature because fusion can be initiated by those particles which are out on the high-energy tail of the Maxwellian distribution of particle energies. The critical ignition temperature is lowered further by the fact

that some particles, which have energies below the coulomb barrier which can tunnel through the barrier.

The presumed height of the coulomb barrier is based upon the distance at which the nuclear strong force could overcome the coulomb repulsion. The required temperature may be overestimated if the classical radii of the nuclei are used for this distance, since the range of the strong interaction is significantly greater than a classical proton radius. With all these considerations, the critical temperatures for the two most important cases are about

$$\text{Deuterium-Deuterium Fusion} : 40 \times 10^7\,\text{K}$$

$$\text{Deuterium-Tritium Fusion} : 4.5 \times 10^7\,\text{K}$$

The tokamak fusion test reactor (TFTR), for example, reached a temperature of 5.1×10^8 K, well above the critical ignition temperature for D-T fusion. TFTR was the world's first magnetic fusion device to perform extensive scientific experiments with plasmas composed of 50/50 deuterium/tritium (D-T), the fuel mix required for practical fusion power production, and also the first to produce more than 10 million watts of fusion power.

The tokamak fusion test reactor (TFTR) was an experimental tokamak built at Princeton Plasma Physics Laboratory (in Princeton, New Jersey) circa 1980. Following on from the Poloidal Diverter Experiment (PDX) and Princeton Large Torus (PLT) devices, it was hoped that TFTR would finally achieve fusion energy breakeven. Unfortunately, the TFTR never achieved this goal. However, it did produce major advances in confinement time and energy density, which ultimately contributed to the knowledge base necessary to build International Thermonuclear Experimental Reactor (ITER). TFTR operated from 1982 to 1997. See Fig. 2.13.

ITER is an international nuclear fusion research and engineering megaproject, which will be the world's largest magnetic confinement plasma experiment. It is an experimental tokamak nuclear fusion reactor, which is being built next to the Cadarache facility in Saint-Paul-lès-Durance, south of France. Figure 2.14 is a depiction of sectional view of ITER comparing to the man scale standing to the lower right of picture.

Therefore, in summary, temperature for fusion that required to overcome the coulomb barrier for fusion to occur is so high to require extraordinary means for their achievement.

$$\text{Deuterium-Deuterium Fusion} : 40 \times 10^7\,\text{K}$$

$$\text{Deuterium-Tritium Fusion} : 4.5 \times 10^7\,\text{K}$$

In the sun, the proton-proton cycle of fusion is presumed to proceed at a much lower temperature because of the extremely high density and high population of particles.

$$\text{Interior of the sun, proton cycle} : 1.5 \times 10^7\,\text{K}$$

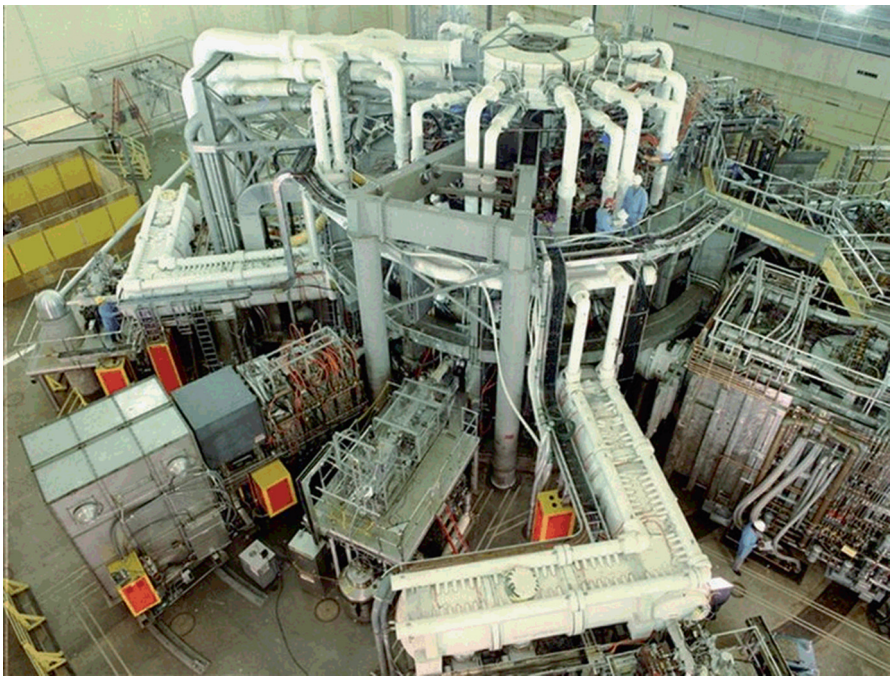

Fig. 2.13 Physical shape of TFTR in Princeton Plasma Physics Laboratory

Fig. 2.14 Sectional view of ITER's tokamak

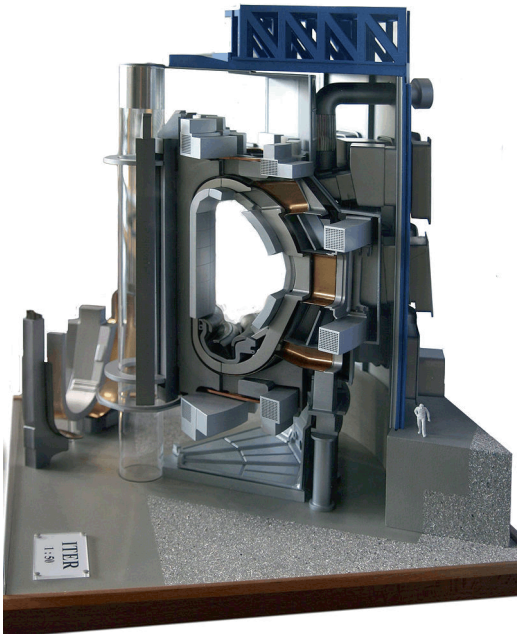

2.8 Controlled Thermonuclear Ideal Ignition Temperature

The minimum operating temperature for a self-sustaining thermonuclear fusion reactor of magnetic confinement type (MCF) is that at which the energy deposited by nuclear fusion within the reacting system just exceeds that lost from the system as a result of Bremsstrahlung emission which is thoroughly described in the next two sections of this chapter here.

To determine its value, it is required to calculate the rates of thermonuclear energy production at a number of temperatures, utilizing Eqs. 2.47 and 2.50 together with Fig. 2.10, for *charged-particle products only*, and to compare the results with the rates of energy loss as Bremsstrahlung derived from the following equations as Eqs. 2.53 and 2.54

$$P_{\mathrm{DD(br)}} = 5.5 \times 10^{-31} n_{\mathrm{D}}^2 T_{\mathrm{e}}^{1/2} \quad \mathrm{W/cm^3} \qquad \text{(Eq. 2.53)}$$

and

$$P_{\mathrm{DT(br)}} = 2.14 \times 10^{-30} n_{\mathrm{D}} n_{\mathrm{T}} T_{\mathrm{e}}^{1/2} \quad \mathrm{W/cm^3} \qquad \text{(Eq. 2.54)}$$

Note that the above two equations are established with assumption that for a plasma consisting only of hydrogen isotopes, $Z = 1$ and n_{i} and n_{e} are equal, so that the factor $n_{\mathrm{e}} \sum (n_{\mathrm{i}} Z^2)$ (this is described later in this chapter under Bremsstrahlung emission rate) may be replaced by n^2 where n is the particle density of either electrons or nuclei.

Note that the factor $n_{\mathrm{e}} \sum (n_{\mathrm{i}} Z^2)$ is sometimes written in the form $n_{\mathrm{e}}^2 \left(\sum n_{\mathrm{e}} Z^2 / \sum n_{\mathrm{i}} Z \right)$, since n_{e} is equal to $\sum n_{\mathrm{i}} Z$.

The assumption that we have made here utilizing both Eqs. 2.53 and 2.54 arises from the fact that, in the plasma, the kinetic ion (nuclear) temperature and the electron temperature are the same.

To illustrate the ideal ignition temperature schematically, we take n_{D} to be as 10^{15} nuclei/cm^3 for the D-D reactions, whereas n_{D} and n_{T} are each 0.5×10^{15} nuclei/cm^3 for the D-T reaction. This makes Bremsstrahlung lose the same for the two cases. The results of the calculations are shown in Fig. 2.15.

The energy rates are expressed in terms of the respective power densities, i.e., energy produced or lost per unit time per unit volume of reaching system. It seems that the curve for the rate of energy loss as Bremsstrahlung intersects the D-T and D-D energy production curves at the temperatures of 4 and 36 keV, i.e., 4.6×10^7 and 4.1×10^8 K, respectively. These are sometime called the *ideal ignition temperature*.

If we assume a Maxwellian distribution of electron velocities, then for rate of Bremsstrahlung energy emission per unit volume, it provides an accurate treatment and equation of for total power radiation P_{br} as

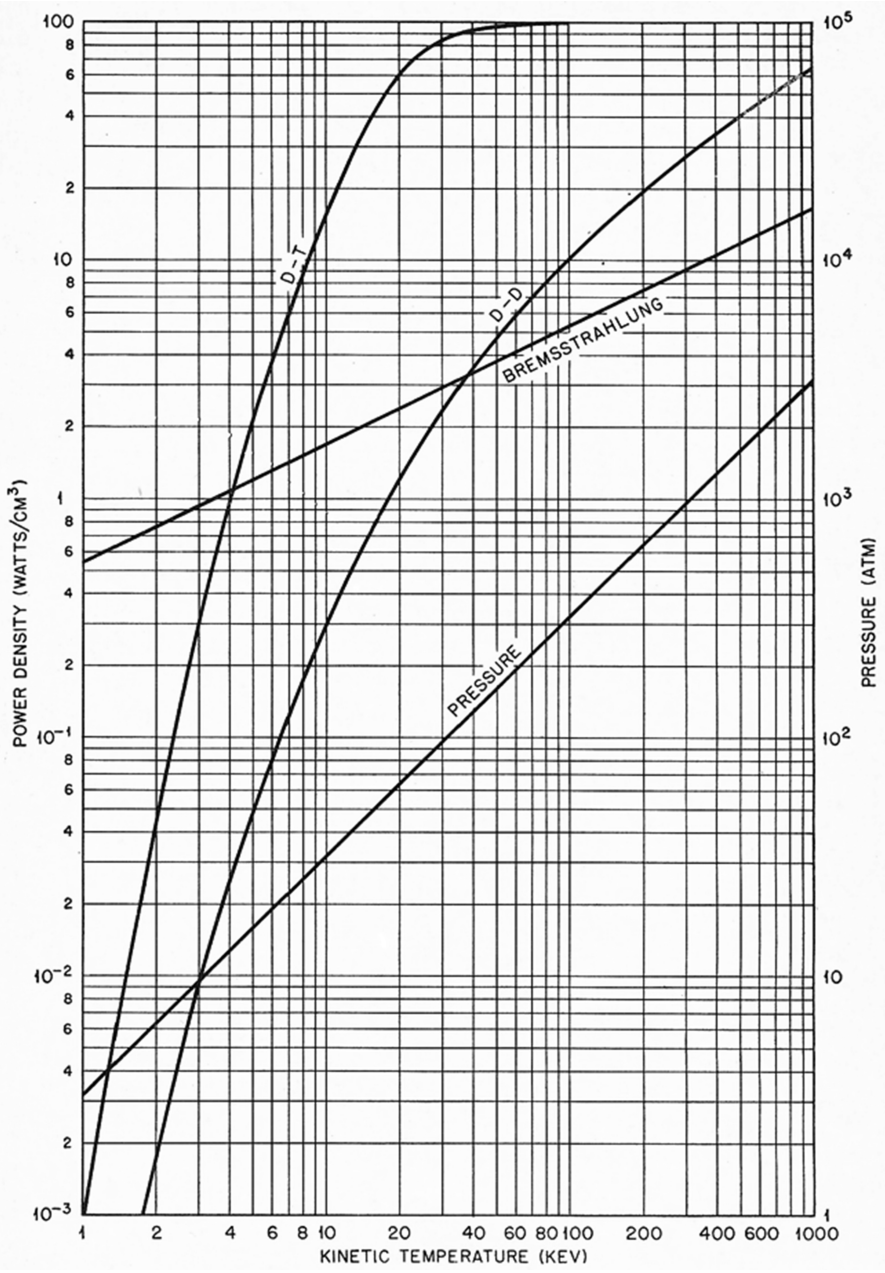

Fig. 2.15 Characteristic of thermonuclear fusion reactions and the ideal ignition temperature [1]

$$P_{\mathrm{br}} = g\frac{32\pi}{3\sqrt{3}} \cdot \frac{(2\pi kT)e^6}{m_{\mathrm{e}}^{3/2}c^3h} n_{\mathrm{e}} \sum n_{\mathrm{i}} Z^2 \qquad \text{(Eq. 2.55)}$$

This equation will be explained later on, in more details, and then the ideal ignition temperature values defined in above are the lowest possible operating temperatures for a self-sustaining thermonuclear fusion reactor. For temperatures lower than the ideal ignition values, the Bremsstrahlung loss would exceed the rate of thermonuclear energy deposition by charged particles in the reacting system.

There exist two other factors, which require the actual plasma kinetic temperature to exceed the ideal ignition temperature vales given above. These are in addition to various losses besides just Bremsstrahlung radiation losses (Sect. 2.10 of this chapter) that we possibly can be minimized, but not completely eliminate in a thermonuclear fusion power plant reactor.

1. We have not yet considered the Bremsstrahlung emission as described later (Sect. 2.11 of this chapter), arising from Coulomb interaction of electrons with the helium nuclei produced in the thermonuclear fusion reactions as it is shown in Fig. 2.20. Since they carry two unit charges, the loss of energy will be greater than for the same concentration of hydrogen isotope ions.
2. At high temperatures that presents in a thermonuclear fusion reactions, the production of Bremsstrahlung due to electron–electron interactions is very distinctive than those resulting from the electron–ion interactions that is considered above. This is a concern, provided that the relativistic effects do not play in the game and there should not be any electron-electron Bremsstrahlung, but at high electron velocities, such is not the case, and appreciable losses can occur from this form of radiation.

In addition to power densities, Fig. 2.15 reveals that the pressures at the various temperatures stages are based on the ideal gas equation $p = (n_{\mathrm{i}} + n_{\mathrm{e}})kT$, where $(n_{\mathrm{i}} + n_{\mathrm{e}})$ is the total number of particles of nuclei and electron, respectively, per cm ^{3} and T is the presentation of kinetic temperature in Kelvin. Under the present condition here, $n_{\mathrm{i}} = n_{\mathrm{e}} = 10^{15}$ particles/cm^3, so that $(n_{\mathrm{i}} + n_{\mathrm{e}}) = 2 \times 10^{15}$.

With k having dimension of erg/K, the values are found in dimension of dynes/cm^2, and the results have been converted to atmospheres assuming 1 atm $= 1.01 \times 10^6$ dynes/cm^2 and then plotted in Fig. 2.15. This figure also shows that the thermonuclear power densities near the ideal ignition temperatures are in the range of 100–1000 W/cm^3, which would be reasonable for continuous reactor operation of a thermonuclear fusion reaction, and that is the reason behind choosing the density values of as 10^{15} nuclei/cm^3 for purpose of reacting particle illustration [1].

It should be noted that although the energy emitted as Bremsstrahlung may be lost as far as maintaining the temperature of the thermonuclear reacting system is concerned, it would not be a complete loss in the operating fusion reactor. Later on in Sect. 2.11, we can demonstrate that the energy distribution of the electron velocities is Maxwellian, or approximately so and dependence of the Bremsstrahlung energy emission on the wavelength or photon energy and related equation can be derived as well [1].

2.9 Bremsstrahlung Radiation

Bremsstrahlung is a German term that means, "braking rays." It is an important phenomenon in the generation of X-rays. In the Bremsstrahlung process, a high-speed electron traveling in a material is slowed or completely stopped by the forces of any atom it encounters. As a high-speed electron approaches an atom, it will interact with the negative force from the electrons of the atom, and it may be slowed or completely stopped. If the electron is slowed down, it will exit the material with less energy. The law of conservation of energy tells us that this energy cannot be lost and must be absorbed by the atom or converted to another form of energy. The energy used to slow the electron is excessive to the atom, and the energy will be radiated as X-radiation of equal energy. In summary, according to German dictionary, "Bremsen" means to "break," and "Strahlung" means "radiation."

If the electron is completely stopped by the strong positive force of the nucleus, the radiated X-ray energy will have an energy equal to the total kinetic energy of the electron. This type of action occurs with very large and heavy nuclei materials. The new X-rays and liberated electrons will interact with matter in a similar fashion to produce more radiation at lower energy levels until finally all that is left is a mass of long wavelength electromagnetic wave forms that fall outside the X-ray spectrum.

Figure 2.16 here is showing Bremsstrahlung effect, produced by a high-energy electron deflected in the electric field of an atomic nucleus.

Characteristics of X-rays are indication that they are emitted from heavy elements when their electrons make transition between the lower atomic energy levels. The characteristic X-ray emission which is shown as two sharp peaks in the illustration at left occur when vacancies are produced in the $n = 1$ or K-shell of the atom and electrons drop down from above to fill the gap. The X-rays produced by transitions from the $n = 2$ to $n = 1$ levels are called K-alpha X-rays, and those for the $n = 3 \rightarrow 1$ transition are called K-beta X-rays. See Fig. 2.17.

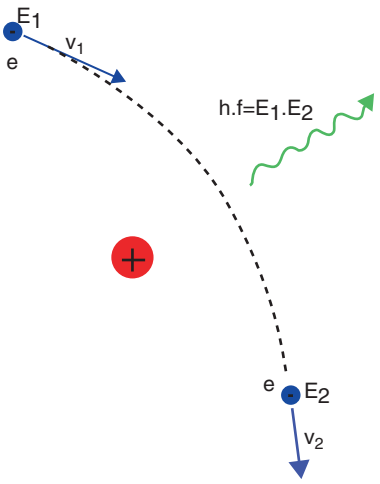

Fig. 2.16 Illustration of Bremsstrahlung effect

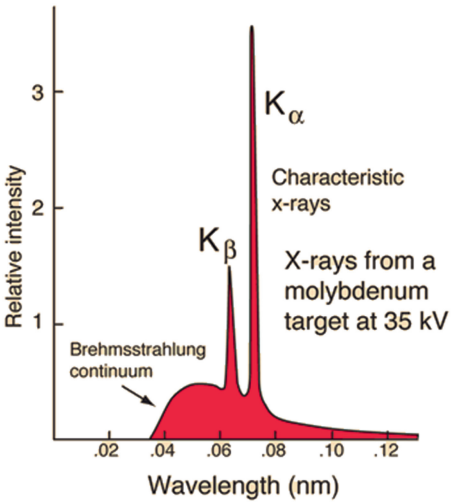

Fig. 2.17 X-rays characteristic illustration

Transitions to the $n = 2$ or L-shell are designated as L X-rays ($n = 3 \rightarrow 2$ is L-alpha, $n = 4 \rightarrow 2$ is L-beta, etc.). The continuous distribution of X-rays which forms the base for the two sharp peaks at left is called "Bremsstrahlung" radiation.

X-ray production typically involves bombarding a metal target in an X-ray tube with high-speed electrons which have been accelerated by tens to hundreds of kilovolts of potential. The bombarding electrons can eject electrons from the inner shells of the atoms of the metal target. Those vacancies will be quickly filled by electrons dropping down from higher levels, emitting X-rays with sharply defined frequencies associated with the difference between the atomic energy levels of the target atoms.

The frequencies of the characteristic X-rays can be predicted from the Bohr model. Moseley measured the frequencies of the characteristic X-rays from a large fraction of the elements of the periodic table and produced a plot of them, which is now called a "Moseley plot" and that plot is shown in Fig. 2.18 here as well for general knowledge purpose.

When the square root of the frequencies of the characteristic X-rays from the elements is plotted against the atomic number, a straight line is obtained. In his early 20s, Moseley measured and plotted the X-ray frequencies for about 40 of the elements of the periodic table. He showed that the K-alpha X-rays followed a straight line when the atomic number Z versus the square root of frequency was plotted. With the insights gained from the Bohr model, we can write his empirical relationship as follows:

$$h\upsilon_{K_\alpha} = 13.6\,\text{eV}(Z-1)^2\left[\frac{1}{1^2}-\frac{1}{2^2}\right] = \frac{3}{4}13.6(Z-1)^2\,\text{eV} \qquad \text{(Eq. 2.56)}$$

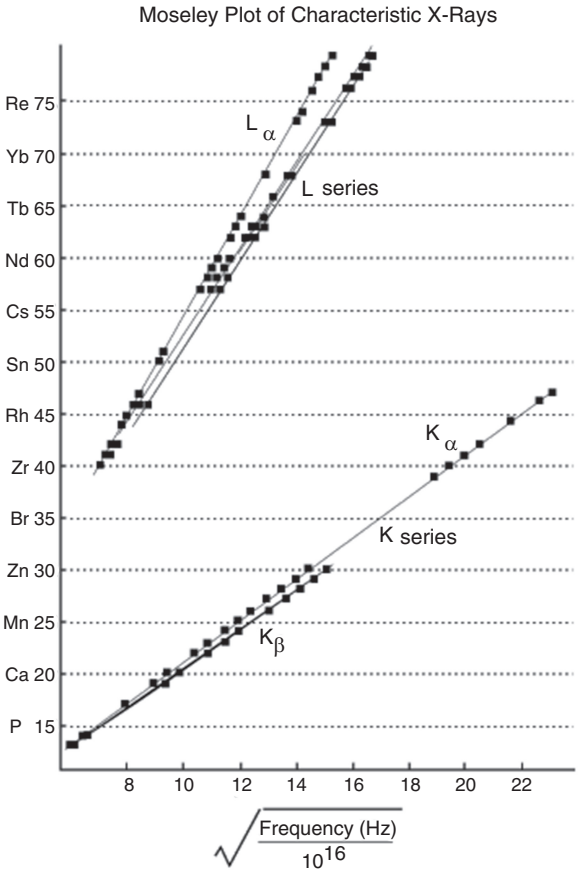

Fig. 2.18 Moseley's plot

Adapted from Moseley's original data (H.G.J.Moseley, Philos. Mag. (6) 27:703, 1914)

Characteristic X-rays are used for the investigation of crystal structure by X-ray diffraction. Crystal lattice dimensions may be determined with the use of Bragg's law in a Bragg spectrometer.

As it was stated above, "Bremsstrahlung" means "braking radiation" and is retained from the original German to describe the radiation, which is emitted when electrons are decelerated or "braked" when they are fired at a metal target. Accelerated charges give off electromagnetic radiation, and when the energy of the bombarding electrons is high enough, that radiation is in the X-ray region of the electromagnetic spectrum. It is characterized by a continuous distribution of radiation, which becomes more intense and shifts toward higher frequencies when the energy of the bombarding electrons is increased. The curves in Fig. 2.19 are from the 1918 data of Ulrey, who bombarded tungsten targets with electrons of four different energies.

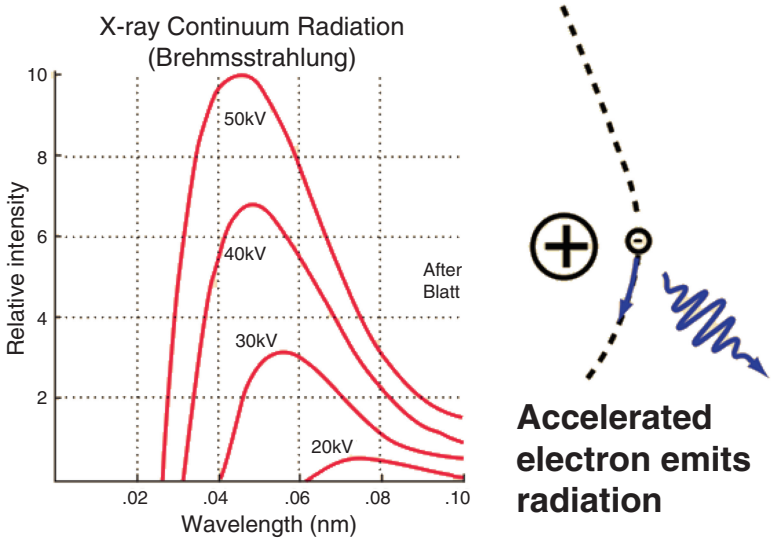

Fig. 2.19 Bremsstrahlung X-ray illustration

The bombarding electrons can also eject electrons from the inner shells of the atoms of the metal target, and the quick filling of those vacancies by electrons dropping down from higher levels gives rise to sharply defined characteristic X-rays.

A charged particle accelerating in a vacuum radiates power, as described by the Larmor formula and its relativistic generalizations. Although the term Bremsstrahlung is usually reserved for charged particles accelerating in matter, not vacuum, the formulas are similar. In this respect, Bremsstrahlung differs from Cherenkov radiation, another kind of braking radiation which occurs only in matter and not in a vacuum.

The total radiation power in most established relativistic formula is given by

$$P = \frac{q^2\gamma^4}{6\pi\varepsilon_0 c}\left[\dot{\beta}^2 + \frac{\left(\vec{\beta}\cdot\dot{\vec{\beta}}\right)^2}{1-\beta^2}\right] \qquad \text{(Eq. 2.57)}$$

where $\vec{\beta} = \vec{v}/c$ which is the ratio of the velocity of the particle divided by the speed of light and $\gamma = \frac{1}{\sqrt{1-\beta^2}}$ is the Lorentz factor, $\dot{\vec{\beta}}$ signifies a time derivation of $\vec{\beta}$, and q is the charge of the particle. This is commonly written in the mathematically equivalent form using

$$\left(\vec{\beta}\cdot\dot{\vec{\beta}}\right)^2 = \vec{\beta}^2\cdot\dot{\vec{\beta}}^2 - \left(\vec{\beta}\times\dot{\vec{\beta}}\right)^2$$
$$P = \frac{q^2\gamma^6}{6\pi\varepsilon_0 c}\left(\dot{\beta}^2 - \left(\vec{\beta}\times\dot{\vec{\beta}}\right)^2\right) \qquad \text{(Eq. 2.58)}$$

In the case where velocity of particle is parallel to acceleration such as a linear motion situation, Eq. 2.58 reduces to

$$P_{a\left|\right|\upsilon} = \frac{q^2a^2\gamma^6}{6\pi\varepsilon_0 c^3} \qquad \text{(Eq. 2.59)}$$

where $a \equiv \dot{\upsilon} = \dot{\beta}\,c$ is the acceleration. For the case of acceleration perpendicular to the velocity $\left(\vec{\beta}\cdot\dot{\vec{\beta}} = 0\right)$, which is a case that arises in circular particle acceleration known as *synchrotron*, the total power radiated reduces to

$$P_{a\perp\upsilon} = \frac{q^2a^2\gamma^4}{6\pi\varepsilon_0 c^3} \qquad \text{(Eq. 2.60)}$$

The total power radiation in the two limiting cases is proportional to $\gamma^4(a\perp\upsilon)$ or $\gamma^6(a|\upsilon)$. Since $E=\lambda mc^2$, we see that the total radiated power goes as m^{-4} or m^{-6}, which accounts for why electrons lose energy to Bremsstrahlung radiation much more rapidly than heavier charged particles (e.g., muons, protons, alpha particles). This is the reason a TeV energy electron-positron collider (such as the proposed International Linear Collider) cannot use a circular tunnel (requiring constant acceleration), while a proton-proton collider (such as the Large Hadron Collider) can utilize a circular tunnel. The electrons lose energy due to Bremsstrahlung at a rate $(m_p/m_e)^4 \approx 10^3$ times higher than protons do.

As a general knowledge here, the nonrelativistic Bremsstrahlung formula for accelerated charges at a rat is given by Larmor's formula. For the electrostatic interaction of two charges, the radiation is most efficient, if one particle is an electron and the other particle is an ion. Therefore, Bremsstrahlung for the nonrelativistic case found the spectral radiation power per electron to be

$$P_v = 2\pi P_\omega = \frac{dE}{dtdv} = \frac{n_i Z^2 e^6}{6\pi^2\varepsilon_0^3 c^3 m_e^2 \upsilon}\ln\left(\frac{b_{max}}{b_{min}}\right) \quad h\nu \ll m_e\upsilon^2 \qquad \text{(Eq. 2.61)}$$

where b_{max} and b_{min} are the maximum and minimum projectile to travel a distance of approximately b, respectively. This distance can be used for projectile impulse duration τ as $\tau = b/\upsilon_0$, where υ_0 is the incoming projectile velocity. Note that, on average, the impulse is perpendicular to the projectile velocity [3].

2.10 Bremsstrahlung Plasma Radiation Losses

Now that we have some understanding of physics of Bremsstrahlung radiation, now we can pay our attention to *Bremsstrahlung plasma radiation losses*. So far our discussion has been referred to the energy or power that might be produced in a thermonuclear fusion reactor. This energy must compete with inevitable losses, and the role of the processes which result in such losses is very crucial in determining the operating temperature of a thermonuclear reactor. Some energy losses can be minimized by a suitable choice of certain design parameters [1], but others are included in the reacting system that can be briefly studied and considered here.

Certainly Bremsstrahlung radiation from electron-ion and electron-neutral collisions can be expected. The radiation intensity outside the plasma region will be a function of various factors inside the plasma region such as the electron "kinetic temperature," the velocity distribution, the plasma opacity, the "emissivity," and the geometry. For example, in case of opacity, if we consider a mass of deuterium so large that it behaves as an optically thick or opaque body as far as Bremsstrahlung is concerned, these radiations are essentially absorbed within the system. Under that assumption, then the energy loss will be given by the blackbody radiation corresponding to existing temperature. Note that even at ordinary temperatures, some D-D reactions will occur, although at an extremely slow rate.

The opacity and emissivity in the microwave region are determined by electron density and collision frequency, both measurable quantities. If strong magnetic field is present, the effects of gyroresonance must also be accounted for in obtaining opacity [4].

Our understanding to date of the effects of non-Maxwellian velocity distributions on the radiation at microwave frequencies is not very complete. However, apparently if the collision frequency is of the order of the viewing frequency, the actual velocity distribution is not very important because of the rapid randomization. For other case, however, which in general are the ones of interest in this subject, there still remains much work to be done [4].

At kinetic temperatures in the region of 1 keV or more, substances of low mass number are not only wholly vaporized and dissociated into atoms, but the latter are entirely stripped of their orbital electrons. In other words, matter is in a state of complete ionization; it consists of a gas composed of positively charged nuclei and an equivalent number of negative electrons, with no neutral particles. With this latter statement in hand, we can define the meaning of completely or fully ionized gas, which is characteristic of plasma as well.

An ionized gaseous system consisting of equivalent numbers of positive ions and electrons, irrespective of whether neutral particles are present or not, is referred to as plasma, in addition to what was said in Chap. 1 for definition of plasma. At sufficiently high temperature, when there are no neutral particles and the ions consist of bare nuclei only, with no orbital electron, the plasma may be said to be completely or fully in ionized state.

We now turn our attention to plasma Bremsstrahlung radiation and to the principle source of radiation from fully ionized plasmas, Bremsstrahlung, with magnetic fields present, cyclotron or synchrotron radiation as it was described in previous section. The spectral range of Bremsstrahlung is very wide and extends from just above the plasma frequency into X-ray continuum for typical plasma range. By contrast, the cyclotron spectrum is characterized by line emission at low harmonics of the Larmor frequency. Similarly, synchrotron spectra from relativistic electron display distinctive characteristic [5].

Moreover, whereas cyclotron and synchrotron radiation can be dealt with classically, the dynamics are treated from relativistic viewpoint in the case of synchrotron radiation, Bremsstrahlung from plasmas, and then have to be interpreted from quantum mechanics perspective, though not usually relativistic. Bremsstrahlung radiation results from electrons undergoing transitions between two states of the continuum in the field of an ion or atom.

If the ions in plasma are not completely stripped, emission of energy will take place in the form of optical or excitation radiation. An electron attached to such an ion can absorb energy, e.g., as the result of a collision with a free electron, and thus be raised to an excited state. When the electron returns to a lower quantum level, the excitation energy is emitted in the form of radiation. This represents a possible source of energy loss from the plasma in a thermonuclear fusion reaction system that is considered as fusion reactor. Hydrogen isotope atoms have only a single electron and are completely stripped at a temperature of about 0.05 keV, so that there is no excitation radiation above this temperature. However, if impurities of higher atomic number are present, energy losses in the form of excitation radiation can become very significant, especially at the lower temperature, while the plasma is being heated and even at temperatures as high as 10 keV [1].

If we ignore impurities in the plasma for time being, we may state that the plasma in a thermonuclear fusion reactor system will consist of completely stripped nuclei of hydrogen isotope with an equal number of electrons at appropriate kinetic temperature. From such a plasma, energy will inevitably be lost in the form of Bremsstrahlung radiation, that is, continuous radiation emitted by charges particle, mainly electrons, as a result of deflection by Coulomb fields of other charged particles. See Fig. 2.20, where in this figure b denotes the impact parameter and angle θ the scattering angle.

While beam energies below the Coulomb barrier prevent nuclear contributions to the excitation process, peripheral collisions have to select in the regime of intermediate-energy Coulomb excitation to ensure the dominance of the electromagnetic interaction. This can be accomplished by restricting the analysis to events at extremely forward scattering angles, corresponding to large impact parameters.

Except possibly at temperature about 50 keV, the Bremsstrahlung from a plasma arises almost entirely from electro–ion interactions as it is shown in Fig. 2.19. Since the electron is free before its encounter with an ion and remains free, subsequently, the transitions are often described as “free-free” absorption phenomena, which also can be seen both in inertial confinement fusion (ICF) and magnetic confinement fusion (MCF) thermonuclear reactions, as well as it is considered in inverse Bremsstrahlung effects, which is the subject of the next section here.

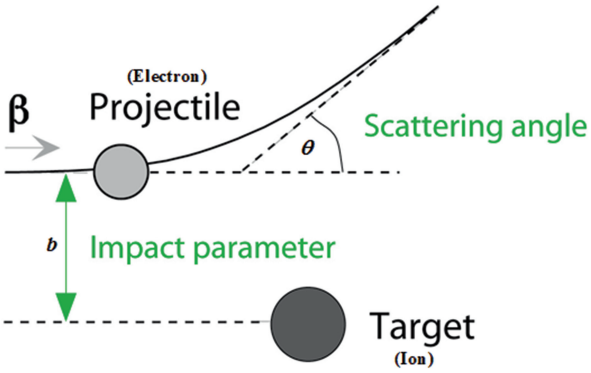

Fig. 2.20 Coulomb scattering between an electron and ion

In theory, the losses due to Bremsstrahlung could be described if the dimensions of the system were larger than the mean free path for absorption of the radiation photons under the existing conditions as it was described before. What these conditions are telling us is that the system or magnetic fusion reactor would be tremendously and impossibly large. This may end up with dimensions as large as 10^6 cm or roughly 600 miles or more, even at very high plasma densities. In a system of this impractical size, a thermonuclear fusion reaction involving deuterium (D) could become self-sustaining without the application of energy from outside source. In other words, a sufficiently large mass of deuterium could attain a critical size, by the propagation of a large thermal chain reaction, just as does a suitable mass of fissionable material as the result of a neutron chain reaction [1].

2.11 Bremsstrahlung Emission Rate

Using a classical expression for the rate P_c at which energy is radiated by an accelerated electron, we can then write

$$P_c = \frac{2e^2}{3c^3}a^2 \qquad \text{(Eq. 2.62)}$$

where:

e = the electric charge
c = the velocity of light
a = the particle acceleration

Per expression presented in Eq. 2.62, we can also make an expression for the rate of electron-ion Bremsstrahlung energy emission of the correct, but differing by a small numerical factor that may be obtained by procedure that is more rigorous.

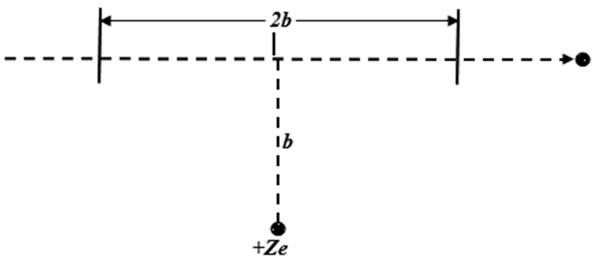

Fig. 2.21 Coulomb interaction of electron with a nucleus

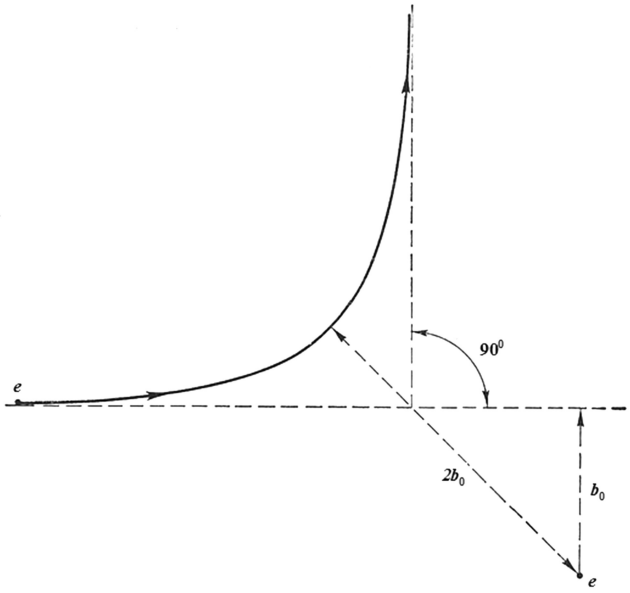

Fig. 2.22 Short-range Coulomb interaction for 90° deflections

If we suppose an electron that moves past a relatively stationary ion of charge Ze with an impact parameter b as we saw in Fig. 2.20 and illustrated in Fig. 2.21 in different depiction as well.

Significance of impact parameter b can be defined in the absence of any electrostatic forces, which is the distance of closest approach between two particles. This will appear as an approximate value of large-angle, single-collision cross section for short-range interaction or close encounter between charged particles may be obtained by a simple, classical mechanics and electromagnetic treatment based on Coulomb's law.

The magnitude of this distance will determine the angle of deflection of one particle by the other. Let for a deflection of 90°, the impact parameter be b_0 as shown in Fig. 2.22 and by making a simplifying assumption that the mass of scattered particle is less than that of scattering particle so that the latter remains

essentially stationary during this encountering. It is found from Coulomb's law that, for 90° deflections, the particles are a distance $2b_0$ apart at the point of closest approach.

From the viewpoint of classical electrodynamics, we see that the mutual potential Coulomb energy is equal to the center of mass or relative kinetic energy E of interacting particles. In the case of a *hydrogen isotope* plasma, all the particles carry the unit charge e, and the mutual potential energy at the point of closest approach is $e^2/2b_0$, and by law of conservation of energy, we can write

$$E = \frac{e^2}{2b_0} \qquad \text{(Eq. 2.63a)}$$

or

$$b_0 = \frac{e^2}{2E} \qquad \text{(Eq. 2.63b)}$$

Now continuing with the beginning of this section and our concern about Bremsstrahlung emission rate, we go on to say that the coulomb force between the charged particles is then Ze^2/b^2. Now let m_e be the electron rest mass; then its acceleration is Ze^2/b^2m_e, and the rate of energy loss as radiation is given by Eq. 2.62 as

$$P_e \approx \frac{2e^6Z^2}{3m_e^2c^3b^4} \qquad \text{(Eq. 2.64)}$$

If we designate, the electron path length over which the Coulomb force is effective with $2b_0$ as it is illustrated in Fig. 2.21, and if the velocity is υ, then the time during which acceleration occurs is $2b/\upsilon$. However, if the acceleration is assumed to be constant during this time, then the total energy E_e radiated as the electron moves past an ion with an impact parameter is written as

$$E_e \approx \frac{4e^6Z^2}{3m_e^2c^3b^3\upsilon} \qquad \text{(Eq. 2.65)}$$

Multiplying Eq. 2.65 by n_e and n_i that are the numbers of electrons and ions, respectively, per unit volume, and also by velocity υ, the result is the rate of energy loss P_a per unit impact area for all ion-electron collisions occurring in unit volume at an impact parameter b, and then we can write

$$P_a \approx \frac{4e^6n_en_iZ^2}{3m_e^2c^3b^3} \qquad \text{(Eq. 2.66)}$$

The total power P_{br} radiated as Bremsstrahlung per unit volume is obtainable upon multiplying Eq. 2.66 by $2\pi bdb$ and integrating over all values of b from $b_{\min}$, the distance of closest approach of an electron to an ion, to infinity; thus, the result would be

$$P_{\mathrm{br}} \approx \frac{8\pi e^6 n_{\mathrm{e}} n_{\mathrm{i}} Z^2}{3m_{\mathrm{e}}^2 c^3 b_{\min}} \int_{b_{\min}}^{b} \frac{db}{b^2} = \frac{8\pi e^6 n_{\mathrm{e}} n_{\mathrm{i}} Z^2}{3m_{\mathrm{e}}^2 c^3 b_{\min}} \qquad \text{(Eq. 2.67)}$$

An estimate of the minimum value of the impact parameter can be made by utilizing the Heisenberg uncertainty principle relationship, i.e.,

$$\Delta x \Delta p \approx \frac{h}{2\pi} \qquad \text{(Eq. 2.68)}$$

when Δx and Δp are the uncertainties in position and momentum, respectively, of a particle and h is Planck's constant. The uncertainty in the momentum may be set to the momentum $m_{\mathrm{e}}\upsilon$ of the electron, and Δx may then be identified with $b_{\min}$, so that

$$b_{\min} \approx \frac{h}{2\pi m_{\mathrm{e}} \upsilon} \qquad \text{(Eq. 2.69)}$$

Furthermore, we assume a Maxwellian distribution of velocity among the electrons; it is possible to write

$$\frac{1}{2} m_{\mathrm{e}} \upsilon^2 = \frac{3}{2} kT_{\mathrm{e}} \qquad \text{(Eq. 2.70)}$$

where T_{e} is the kinetic temperature of the electrons; hence,

$$b_{\min} \approx \frac{h}{2\pi (3kT_{\mathrm{e}} m_{\mathrm{e}})^{1/2}} \qquad \text{(Eq. 2.71)}$$

Substituting Eq. 2.71 into Eq. 2.67, the result would be

$$P_{\mathrm{br}} \approx \frac{16\pi^2}{3^{1/2}} \cdot \frac{(kT_{\mathrm{e}})^{1/2} e^6}{m_{\mathrm{e}}^{3/2} c^3 h} n_{\mathrm{e}} n_{\mathrm{i}} Z^2 \qquad \text{(Eq. 2.72)}$$

Equation 2.72 refers to a system containing a single ionic species of charge Z. In the case of a mixture of the ions or nuclei, it is obvious that the quantity $n_{\mathrm{i}}Z^2$ should be replaced by $\sum(n_{\mathrm{i}}Z^2)$, where the summation is taken over all the ion present. Note that the factor $n_{\mathrm{e}} \sum (n_{\mathrm{i}} Z^2)$ is sometime written in the form $n_{\mathrm{e}}^3 \left(\sum n_{\mathrm{e}} Z^3 / \sum n_{\mathrm{i}} Z \right)_{\mathrm{i}}$, since n_{e} is equal to $\sum n_{\mathrm{i}} Z$. This was mentioned in Sect. 2.8 of this chapter as well.

As we mentioned above and presented in Eq. 2.55, a more precise treatment, assuming Maxwellian distribution of electron velocities, gives for the rate of Bremsstrahlung energy emission per unit volume and write same equation again.

$$P_{\mathrm{br}} = g\frac{32\pi}{3\sqrt{3}} \cdot \frac{(2\pi kT)^{1/2} e^6}{m_{\mathrm{e}}^{3/2} c^3 h} n_{\mathrm{e}} \sum n_{\mathrm{i}} Z^2 \qquad \text{(Eq. 2.73)}$$

where g is the Gaunt factor which corrects the classical expression for the requirements of quantum mechanics. At high temperatures, the correction factor approaches a limiting value of $2 \times 3^{1/2}/\pi$**;** and taking this result together with the known values of Boltzmann constant k in erg/K, e is statcoulombs; and m_{e}, c, and h in cgs units, as in Eq. 2.73 or exact equation that is written in Eq. 2.55, become

$$P_{\mathrm{br}} = 1.57 \times 10^{-27} n_{\mathrm{e}} \sum \left(n_{\mathrm{i}} Z^2\right) T_{\mathrm{e}}^{1/2} \,\mathrm{ergs}/\left(\mathrm{cm}^3\,\mathrm{s}\right) \qquad \text{(Eq. 2.74)}$$

where T_{e} is the electron temperature in K, or making use of the conversion factor given as T_{e} keV is equivalent to $1.16 \times 10^7\ T_{\mathrm{e}}$ K, where 1 keV $= 1.16 \times 10^7$ K.

The classical expression for the rate of Bremsstrahlung emission per unit volume frequency interval in the frequency range from v to $v + dv$ is given as

$$dP_v = g\frac{32\pi}{3^{3/2}} \left(\frac{2\pi}{kT}\right)^{1/2} \frac{e^6}{m_{\mathrm{e}}^{3/2}} \sum \left(n_{\mathrm{i}} Z^2\right) \exp(-kv/kT) dv \ \mathrm{W}/\left(\mathrm{cm}^3\,\mathrm{angstrom}\right) \qquad \text{(Eq. 2.75)}$$

If we integrate Eq. 2.75 over all frequencies, this expression leads to either Eq. 2.55 or Eq. 2.73, and for our purpose, it is more convenient to express Eq. 2.75 in unit wavelength in the interval from λ to $\lambda + d\lambda$, and that is

$$dP_\lambda = 6.01 \times 10^{-30} g n_{\mathrm{e}} \sum \left(n_{\mathrm{i}} Z^2\right) T_{\mathrm{e}}^{-1/2} \lambda^{-2} \exp(-12.40/\lambda T_{\mathrm{e}}) d\lambda \qquad \text{(Eq. 2.76)}$$

where the temperature is in kilo-electron volts (keV) and the wave lengths are in angstrom.

If we assume the Gaunt factor g to remain constant, as it is not strictly correct, the relative values of $dP_\lambda/d\lambda$ obtained from Eq. 2.76, for arbitrary electron and ion densities, have been plotted as a function of wavelength as it can be seen in Fig. 2.23 for electron temperature of 1, 10, and 100 keV. It can be observed that each curve passes through a maximum at a wavelength in which differentiation of Eq. 2.76 shows to be equal to $6.20/T_{\mathrm{e}}$ angstroms.

Note that to the left of the maximum, the energy emission as Bremsstrahlung is dominated by the exponential term and decreases rapidly with decreasing wavelength. To the right of the maximum, however, the variation approaches a dependence upon $1/\lambda_2$, and the energy emission falls off more slowly with increasing wavelength of the radiation [1].

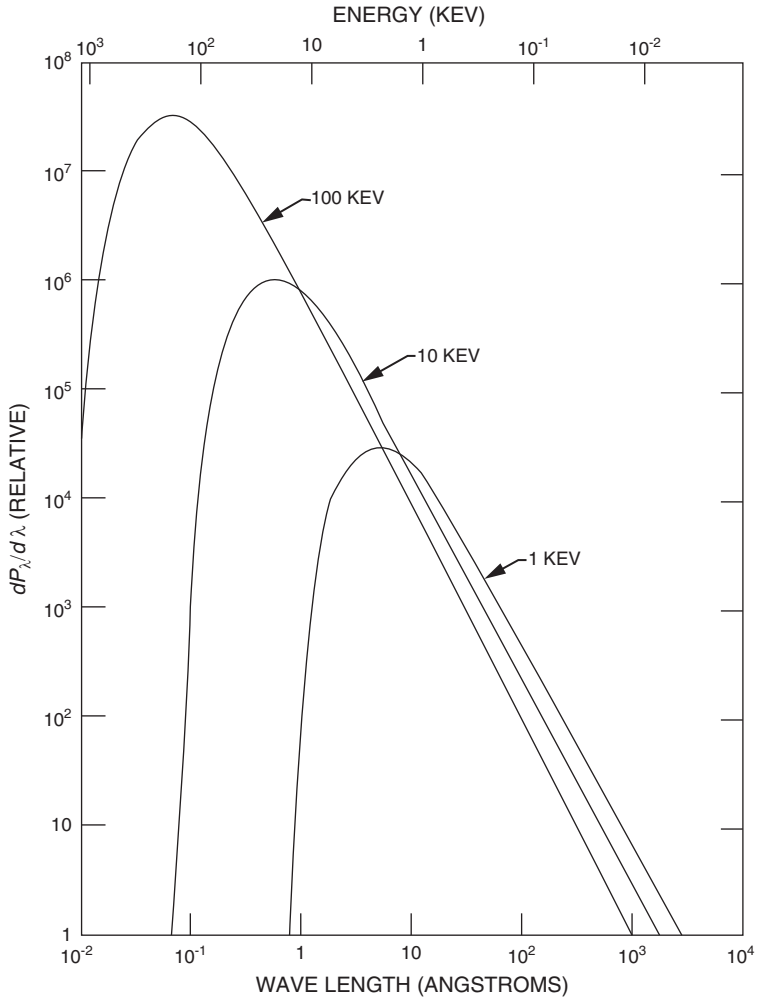

Fig. 2.23 Bremsstrahlung power distribution at kinetic temperature of 1, 10, and 100 keV

2.12 Additional Radiation Losses

As we briefly describe in Sect. 2.8, in addition to various losses apart from Bremsstrahlung radiation loss, which can be minimized but not completely eliminated or contained in a practical reactor, there were two other factors, which were affecting such additional losses. To further enhance these concerns and consider them for prevention of energy losses, we look at the following sources of energy losses.

According to Eq. 2.73, the rate of energy loss as Bremsstrahlung increases with the ionic charge Z, which is equal to the atomic number in a fully ionized gas consisting only of nuclei and electrons. Consequently, the presence of impurities of moderate and high atomic number is thermonuclear reactor system which will increase the energy loss, and as a result, the minimum kinetic temperature at which there is a net production of energy will also be increased [1].

However, if we consider a fully ionized plasma mixture containing n_1 nuclei/cm^3 of hydrogen isotopes ($Z = 1$) and n_e nuclei/cm^3 of an impurity of atomic number Z, then the electron density n_e is $n_1 + n_e Z$ per cm^3. Thus, the factor $n_e \sum (n_i Z^2)$ in Eq. 2.67 needs to be equal to $(n_1 + n_z Z)(n_1 + n_z Z^2)$. In the absence of the impurity, thus, the corresponding factor would be n_1^2. This follows that, from Eq. 2.75, we can write

$$\frac{\text{Power Loss in the Presence of Impurity}}{\text{Power Loss in the Absence of Impurity}} = \frac{(n_1 + n_z Z)\left(n_1 + n_z Z^2\right)}{n_1^2} = 1 + f^2 Z^2 + fZ(Z+1) \qquad \text{(Eq. 2.77)}$$

where $f = n_e/n_1$, i.e., the fraction of impurity atoms.

Glasstone and Lovberg [1] argue that if the impurity, for example, is oxygen with atomic number $Z = 8$ and that is present to the extent of 1 at.%, so that $f = 0.01$, then in that case, Eq. 2.77 results in the following value as

$$\frac{\text{Power Loss in the Presence of Impurity}}{\text{Power Loss in the Absence of Impurity}} = 1.77 \qquad \text{(Eq. 2.78)}$$

In words what Eq. 2.78 is telling us is that the presence of only 1 at.% of oxygen impurity will increase the rate of energy loss as Bremsstrahlung by 77%. In the case of the D-D reaction system, Fig. 2.15 shows this would raise the ideal ignition temperature from 36 to 80 keV, and for D-T reaction, the same temperature increases from 4 to 4.5 keV.

To remind again that "ideal ignition temperature is the minimum operation temperature for a self-sustaining thermonuclear reactor is that at which the energy deposited by nuclear fusion within the reacting system just exceeds that lost from the system as a result of Bremsstrahlung emission" [1].

Per statement and example in above, it is obvious for a thermonuclear reactor system with impurity of higher atomic number, the increase on ideal ignition temperature extremely would be high; thus, it appears to be an important requirement of a thermonuclear fusion reactor that even traces impurities, especially those of the moderate and high atomic number. Therefore, such impurities should be rigorously excluded from the reacting plasma, and there might be some possible exception to this rule [1].

To remind ourselves of an imperfect ionized impurity of plasma, we can also claim the following statement as well.

Imperfectly ionized impurity atoms with medium to high atomic number incur additional radiation losses in a plasma reactor. Electrons lose energy if these ions are further ionized or excited. This energy is then the radiation from the plasma when later on an electron is captured, mainly recombination radiation, or when, ion returns to its original state, then radiation loss is via line radiation, respectively. Energy losses P_e^{LR} from both sources can be written in general form of

$$P_e^{LR} = -n_e \sum_{\sigma} n_\sigma f_\sigma(T_e) \qquad \text{(Eq. 2.79)}$$

where f_σ is a complicated function of T_e. Both line and recombination losses may exceed Bremsstrahlung losses by several orders of magnitude. As we talked about cyclotron effect in magnetic confinement of plasma, radiation from gyrating electrons also represents a loss source. Calculation of this one is very difficult in view of the fact that this radiation is partly reabsorbed in the plasma and partly reflected by the surrounding walls of reactor. Fortunately, it is small compared with Bremsstrahlung losses under typical reactor conditions [6].

Note that recombination radiation is caused by *free-bound* transition. To elaborate further, we look at the final state of the electron that is a bound state of the atom or ion, if the ion was initially multiplied and ionized. The kinetic energy of the electron together with the difference in energy between the final quantum state n and the ionization energy of the atom or ion will appear as photon energy. This event involving electron capture is known as *radiative recombination* and emission as *recombination radiation*. In certain circumstances, recombination radiation may dominate over Bremsstrahlung radiation.

Other losses arise from energy exchange between components having different temperatures and from the interaction with the ever present neutral gas background, namely, ionization and charge exchange. The study of these terms beyond the scope of this book and readers can refer to a textbook by Glasstone and Lovberg [1] as well as Raeder et al. [6].

2.13 Inverse Bremsstrahlung in Controlled Thermonuclear ICF and MCF

In case of laser-driven fusion, we have to be concerned by the dense plasma heating by inverse Bremsstrahlung, and it is very crucial for the design and critical evaluation of target for inertial confinement fusion (ICF) to thoroughly understand the interaction of the laser radiation with dense, strongly coupled plasmas.

To accommodate the symmetry conditions needed, the absorption of laser energy must be carefully determined starting from the early stages [7, 8]. The absorption data for dense plasmas are also required for fast ignition by ultra-intense lasers due to creation of plasmas by the nanosecond pre-pulse [9]. Least understood

are laser-plasma interactions that involve strongly coupled $\Gamma > 1$ and partially degenerate electrons. Such conditions also occur in warm dense matter experiments [10, 11] and laser cluster interactions [12, 13].

The dominant absorption mechanism for lasers with the parameters typical for inertial confinement fusion is inverse Bremsstrahlung. Dawson and Oberman [14] first investigated this problem for weak fields. Decker et al. [15] later extended their approach to arbitrary field strengths. However, due to the use of the classical kinetic theory, their results were inapplicable for dense, strongly coupled plasmas. This problem was addressed using a rigorous quantum kinetic description applying the Green's function formalism [16, 17] or the quantum Vlasov approach [18]. However, these approaches are formulated in the high-frequency limit, which requires the number of electron-ion collisions per laser cycle to be relatively small. In the weak field limit, a linear response theory can be applied, and thus the strong electron-ion collisions were also included into a quantum description [19, 20] in this limit.

For dense strongly coupled plasmas, the approach for the evaluation of the laser absorption in both the high- and low-frequency limits must be fundamentally different. In the high-frequency limit, the electron-ion interaction has a collective rather than a binary character, and the laser energy is coupled into the plasmas via the induced polarization current. On the other hand, binary collisions dominate laser absorption in the low-frequency limit resulting in a Drude-like formulation. At the intermediate frequencies, both strong binary collisions and collective phenomena have to be considered simultaneously. Interestingly, such conditions occur for moderate heating at the critical density of common Ny:Yag lasers.

Inverse Bremsstrahlung absorption in inertial fusion confinement (ICF) or laser-driven fusion is an essential and fundamental mechanism for coupling laser energy to the plasma. Absorption of laser light at the ablation surface and critical surface of the pellet of D-T as target takes place via inverse Bremsstrahlung phenomenon in the following way:

- Laser intensity at the ablation surface causes the electrons to oscillate and consequently induced an electric field. Created energy due to the above oscillation of electrons will be converted into thermal energy via electron-ion collisions, which is known as inverse Bremsstrahlung process.

Bremsstrahlung and its inverse phenomena are linked in the following way:

- If two charged particles undergo a Coulomb collision as it was discussed before, they emit radiation, which is called again Bremsstrahlung radiation. Therefore, inverse Bremsstrahlung radiation is the opposite process, where electron scattered in the field of an ion absorbed a photon.

Note that b in Fig. 2.24 denotes the impact parameters that are defined before, and θ is the scattering angle.

Using the notation as given in Fig. 2.24, the differential cross section $d\sigma_{ei}/d\Omega$ for such a coulomb collision is described by Rutherford formula as follows:

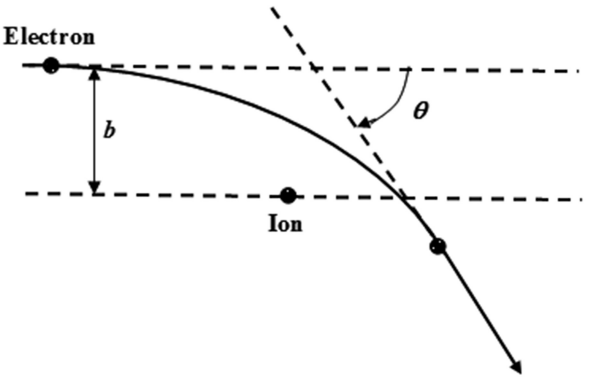

Fig. 2.24 Coulomb scattering between an electron and ion

$$\frac{d\sigma_{ei}}{d\Omega} = \frac{1}{4}\left(\frac{Ze^2}{m_e v^2}\right)^2 \frac{1}{\sin^4(\theta/2)} \qquad \text{(Eq. 2.80)}$$

where:

θ = the scattering angle
Ω = the differential solid angle

If we consider our analysis within spherical coordinate system, then the solid angle Ω is presented as

$$d\Omega = 2\pi \sin\theta d\theta \qquad \text{(Eq. 2.81)}$$

In same coordinate, the impact parameter b is related to the scattering angle θ via the following formula as

$$\tan\left(\frac{\theta}{2}\right) = \frac{Ze^2}{m_e v^2 b} \qquad \text{(Eq. 2.82)}$$

By the substitution of Eqs. 2.81 and 2.82 along with utilization of Eq. 2.80, we can now find the total cross section σ_{ei} for electron-ion collisions by integrating overall possible scattering angle, and that is give as

$$\sigma_{ei} = \int \frac{d\sigma_{ei}}{d\Omega} d\Omega = \frac{\pi}{2}\left(\frac{Ze^2}{m_e v^2}\right)^2 \int_0^{\pi} \frac{\sin\theta}{\sin^4(\theta/2)} d\theta \qquad \text{(Eq. 2.83)}$$

The integral from $\theta \to 0$ to $\theta \to \pi$, which is equivalent to $b \to \infty$ and $b \to 0$ diverges. However, in plasma, the condition allows for us to define a lower and upper boundary limit b_{min} and b_{max}, respectively, and for that matter, the integration in Eq. 2.83 reduces to the following form as

$$\sigma_{ei} = \frac{\pi}{2}\left(\frac{Ze^2}{m_e v^2}\right)^2 \int_{b_{min}}^{b_{max}} \frac{\sin\theta}{\sin^4(\theta/2)} d\theta \qquad \text{(Eq. 2.84)}$$

The upper limit of this integral arises from Debye shielding that is defined in Chap. 1 of this book, which makes collision distance ineffective. Therefore, in a plasma, the b_{max} limit can be replaced by Debye length λ_D. However, the lower limit b_{min} is often set to be equal to the Broglie wavelength, which Lifshitz and Pitaevskii [21] have shown that this approach is not adequate and they derived the lower limit to be $b_{min} = Ze^2/k_B T_e$. Now that we have established lower and upper bound limit, Eq. 2.84 reduces to the following form in order to show the total cross section σ_{ei} in a plasma by

$$\sigma_{ei} = \frac{\pi}{2}\left(\frac{Ze^2}{m_e v^2}\right)^2 \int_{Ze^2/k_B T_e}^{\lambda_D} \frac{\sin\theta}{\sin^4(\theta/2)} d\theta \qquad \text{(Eq. 2.85)}$$

Thus, having the knowledge of the cross section via Eq. 2.85, one can calculate the collision frequency ν_{ei} in the plasma. However, the collision frequency ν_{ei} is defined as the number of collision, and electron undergoes with the background ions in plasma per unit time, and it depends on the ion density n_i, the cross section σ_{ei}, and the electron velocity v_e.

$$\nu_{ei} = n_i \sigma_{ei} v_e \qquad \text{(Eq. 2.86)}$$

In order to calculate the collision frequency ν_{ei}, we need to take the velocity distribution v_e of the particles into account. In many cases, it can be assumed that the ions are at rest ($T_i = 0$) and electrons are in local thermal equilibrium. A Maxwellian electron velocity distribution, v_e, is in the form of the following relation.

$$f(v_e) = \frac{1}{(2\pi k_B T_e/m)^{3/2}} \exp\left[-\left(\frac{m_e v_e^2}{2k_B T_e}\right)\right] \qquad \text{(Eq. 2.87)}$$

is isotropic and normalized in a way that

$$\int_0^\infty \frac{1}{(2\pi k_B T_e/m)^{3/2}} \exp\left[-\left(\frac{m_e v_e^2}{2k_B T_e}\right)\right] = 1 \qquad \text{(Eq. 2.88)}$$

Using Eqs. 2.83 and 2.88 as well as performing the integrations, the electron-ion collision frequency results in

$$\nu_{ei} = \left(\frac{2\pi}{m_e}\right)^{1/2} \frac{4Z^2 e^4 n_i}{3(k_B T_e)^{3/2}} \ln\Lambda \qquad \text{(Eq. 2.89)}$$

where $\Lambda = b_{\max}/b_{\min}$ and the factor Λ is called the Coulomb logarithm, a slowly varying term resulting from the integration over all scattering angles. In case of low-density plasmas and moderate laser intensities driving the fusion reaction, its value typically lies in the range of 10^{-20}.

In order to derive Eq. 2.89, the assumption was made on the fact that small-angle scattering events dominated, which is a valid assumption if the plasma density is not too high. For dense and cold plasma, Eq. 2.89 is not applicable due to large-angle deflections becoming increasingly likely violating the small-angle scattering assumption. If one uses the above-stated method, the values of $b_{\min}$ and $b_{\max}$ can become comparable, so that $\ln\Lambda$ eventually turns negative, which is an obviously unphysical results.

In practical calculations, a lower limit of $\ln\Lambda = 2$ is often assumed; however, for dense plasmas, a more complex treatment needs to be applied which is published by Bornath et al. [22] and Pfalzner and Gibbon [23].

Note that we need to be cautious if the laser intensity is very high, as in this case strong deviations from the Maxwell distribution can occur.

Readers can find more details in the book by Pfalzner [24].

Now that we have briefly analyzed the inverse Bremsstrahlung absorption for inertial fusion confinement (ICF) where laser drives fusion, we now pay our attention to this inverse event from physics of plasma point of view and consider the inverse Bremsstrahlung under free-free absorption conditions.

Free-free absorption inverse Bremsstrahlung takes place when an electron in continuum absorbs a photon. Its macroscopic equivalent is the collisional damping of electromagnetic waves. For a plasma in local thermal equilibrium, having found the Bremsstrahlung emission, we may then refer to Kirchhoff's law to find the free-free absorption coefficient α_ω. As we have stated before, the Bremsstrahlung emission coefficient is represented in terms of the Gaunt factor as an approximation in form of

$$\varepsilon_\omega(T_e) = \frac{8}{3\sqrt{3}} \frac{Z^2 n_e n_i}{m^2 c^3} \left(\frac{e^2}{4\pi\varepsilon_0}\right)^3 \left(\frac{m}{2\pi k_B T_e}\right)^{1/2} \bar{g}(\omega, T_e) e^{-\hbar\omega/k_B T_e} \qquad \text{(Eq. 2.90)}$$

where $\bar{g}(\omega, T_e)$ is defined as

$$\bar{g}(\omega, T_e) = \frac{\sqrt{3}}{\pi} \ln\left|\frac{2m}{\zeta\omega} \frac{4\pi\varepsilon_0}{Ze^2} \left(\frac{2k_B T_e}{\zeta m}\right)^{1/2}\right| \qquad \text{(Eq. 2.91)}$$

From Eq. 2.90, we can see that the Gaunt factor is relatively slowly varying function of $\hbar\omega/k_B T_e$ over a wide range of parameters which means that the dependence of Bremsstrahlung emission on frequency and temperature is largely governed by the factor $(m/2\pi k_B T_e)^{1/2} \exp(-\hbar\omega/k_B T_e)$ in Eq. 2.90. As it also was stated, for laboratory plasmas with electron temperatures in the keV range, the Bremsstrahlung spectrum extends into the X-ray region of the spectrum. Note that the factor $\sqrt{3}/\pi$ in Eq. 2.91 is to conform with the conventional definition of the Gaunt in the quantum mechanical treatment.

In terms of the Rayleigh-Jeans limit, this gives a relationship for free-free absorption coefficient as follows:

$$\alpha_\omega(T_e) = \frac{64\pi^4}{3\sqrt{3}} \frac{Z^2 n_e n_i}{m^3 c\omega^2} \left(\frac{e^2}{4\pi\varepsilon_0}\right) \left(\frac{m}{2\pi k_B T_e}\right)^{1/2} \bar{g}(\omega, T_e) \qquad \text{(Eq. 2.92)}$$

In Eq. 2.91, $\ln\zeta = 0.577$ is Euler's constant, and the factor $(2/\zeta) \simeq 1.12$ in the argument of the logarithm has been included to make $\bar{g}(\omega, T_e)$ in Eq. 2.91 to agree with the exact low-frequency limit determined from the plasma Bremsstrahlung spectrum. Classical picture of plasma Bremsstrahlung spectrum in exact form is the treatment of an electron moving in the Coulomb field of an ion which is a standard problem in classical electrodynamics. Provided the energy radiated as Bremsstrahlung is a negligibly small fraction of the electron energy where the ion is treated as a stationary target, then the electron orbit is hyperbolic, and the power spectrum $dp(\omega)/d\omega$ from a test electron colliding with plasma ions of density n_i may be written as

$$\frac{dp(\omega)}{d\omega} = \frac{16\pi}{3\sqrt{3}} \frac{Z^2 n_i}{m^2 c^3} \left(\frac{e^2}{4\pi\varepsilon_0}\right) \frac{1}{\upsilon} G(\omega b_0/\upsilon) \qquad \text{(Eq. 2.93)}$$

where $b_0 = Ze^2/4\pi\varepsilon_0 m\upsilon^2$ is the impact parameter for 90° scattering, υ is the incident velocity of the electron, and $G(\omega b_0/\upsilon)$ is a dimensionless factor that is known as Gaunt factor as it was defined before, which varies only weakly with plasma frequency ω.

It can be shown that the dispersion relation for electromagnetic waves in an isotropic plasma becomes

$$\frac{c^2 k^2}{\omega^2} = 1 - \frac{\omega_p^2}{\omega(\omega - i\nu_{ei})} \qquad \text{(Eq. 2.94)}$$

This is allowable phenomenologically for the effects of electron-ion collisions through a collision frequency ν_{ei}. Further on, it can be shown that electromagnetic waves are damped as a result of electron-ion collisions, with damping coefficient $\gamma = \nu_{ei}\left(\omega_p^2/2\omega^2\right)$.

If we take Eq. 2.94 into consideration, which is expressing the collision damping of electromagnetic waves, and use this to obtain the absorption coefficient, we provided in Eq. 2.90 the Coulomb logarithm in place of the Maxwell averaged Gaunt factor, a difference that reflects the distinction between these separate approaches. Whereas inverse Bremsstrahlung is identified with incoherent absorption of photon by thermal electrons, the result in Eq. 2.94 is macroscopic in that it derives from a transport coefficient, namely, the plasma conductivity [25].

At the macroscopic level, electron momentum is driven by an electromagnetic field before being dissipated by means of collisions with ions. However, absorption of radiation by inverse Bremsstrahlung as expressed in Eq. 2.92 is more effective at

high densities, low electron temperature, and low-frequency plasmas. For the efficient absorption of laser light by plasma at the ablation surface of target pellet of D-T, the mechanism of the process is very important. We anticipate absorption to be strongest in the region of the critical density n_c, since this is the highest density to which incident light can penetrate. In the vicinity of the critical density $Zn_e n_i \sim n_c^2 = (m\varepsilon_0/e^2)^2 \omega_L^4$, where ω_L is presenting the frequency of the laser light, so that free-free absorption is sensitive to the wavelength of the incident laser light [25].

References

1. S. Glasstone, R.H. Lovberg, *Controlled Thermonuclear Reactions* (D. Van Nostrand Company, Inc., New York, 1960)
2. B. Zohuri, P. McDaniel, *Thermodynamics In Nuclear Power Plant Systems* (Springer International Publishing, Cham, 2015)
3. F. Chen, *Introduction to Plasma Physics and Controlled Fusion*, 3rd edn. (Springer International Publishing, Cham, 2015)
4. J.E. Drummond, *Plasma Physics* (Dover, Mineola, 2013)
5. T.J.M. Boyed, J.J. Sanderson, *The Physics of Plasmas* (Cambridge University Press, Cambridge, 2003)
6. J. Raeder, K. Borrass, R. Bunde, W. Dänner, R. Klingelhöfer, L. Lengyel, F. Leuterer, M. Söll, *Controlled Nuclear Fusion, Fundamentals of Its Utilization for Energy Supply* (Wiley, Chichester, 1986)
7. J.D. Lindl et al., Phys. Plasmas **11**, 339 (2004)
8. M. Michel et al., Phys. Rev. Lett. **102**, 025004 (2009)
9. M.H. Key, Phys. Plasmas **14**, 055502 (2007)
10. A.L. Kritcher et al., Science **322**, 69 (2008)
11. E. Garcia Saiz et al., Nat. Phys. **4**, 940 (2008)
12. B.F. Murphy et al., Phys. Rev. Lett. **101**, 203401 (2008)
13. T. Bornath et al., Laser Phys. **17**, 591 (2007)
14. J.M. Dawson, C. Oberman, Phys. Fluids **5**, 517 (1962)
15. C.D. Decker et al., Phys. Plasmas **1**, 4043 (1994)
16. D. Kremp et al., Phys. Rev. E **60**, 4725 (1999)
17. T. Bornath et al., Phys. Rev. E **64**, 026414 (2001)
18. H.J. Kull, L. Plagne, Phys. Plasmas **8**, 5244 (2001)
19. H. Reinholz et al., Phys. Rev. E **62**, 5648 (2000)
20. A. Wierling et al., Phys. Plasmas **8**, 3810 (2001)
21. E.M. Lifshitz, L.P. Pitaevskii, *Physical Kinetics* (Pergamon Press, Oxford, 1981)
22. T. Bornath, M. Schlanges, P. Hillse, D. Kremp, Phys. Rev. E **64**, 026414 (2001)
23. S. Pfalzner, P. Gibbon, Phys. Rev. E **57**, 4698 (1998)
24. S. Pfalzner, *An Introduction to Inertial Confinement Fusion* (Taylor and Francis, New York, 2006)
25. T.J.M. Boyd, J.J. Sanderson, *The Physics of Plasmas* (Cambridge University Press, Cambridge, 2005)

http://www.springer.com/978-3-319-51176-4

Magnetic Confinement Fusion Driven Thermonuclear Energy

Zohuri, B.

2017, XVI, 185 p. 92 illus., 36 illus. in color., Hardcover
ISBN: 978-3-319-51176-4